

Spatio-temporal variability of zooplankton standing stock in eastern Arabian Sea inferred from ADCP backscatter measurements

Ranjan Kumar Sahu, D. Shankar, P. Amol, S.G. Aparna, D.V. Desai

November 8, 2024

Abstract

We use acoustic Doppler current profiler (ADCP) backscatter measurements to map the spatio-temporal variation of zooplankton standing stock in the eastern Arabian Sea (EAS). The ADCP moorings were deployed at seven locations on the continental slope off the west coast of India; we use data from October 2017 to December 2023. The 153.3 kHz ADCP uses backscatter from sediments or organisms such as copepods, ctenophores, salps and amphipods greater than 1 cm to calculate current profile. The backscatter is obtained from echo intensity using RSSI conversion factor after doing necessary calibrations. The conversion from backscatter to biomass is based on volumetric zooplankton sampling at the respective locations. Analysis of the data over 24–120 m shows that the backscatter and zooplankton biomass decrease from the upper ocean (215 mg^{-3} biomass contour) to the lower depths. Changes are observed in the seasonal variation of the monthly

¹² climatology of zooplankton standing stock (integral of the biomass over 24–120 m water column)
¹³ as we move to poleward along the slope in EAS. The range of variation of standing stock is lowest
¹⁴ at Kanyakumari, followed by Okha, which lie at the southern and northern boundary of the EAS,
¹⁵ respectively. Complementary variables are used to explain the processes leading to growth or decay
¹⁶ of zooplankton biomass. While annual cycle is predominant at NEAS, it decreases towards SEAS
¹⁷ where the semi-annual cycle tends to dominate. Analysis reveals weak presence of annual cycle in
¹⁸ zooplankton biomass and it is dominated by intraseasonal and intra-annual components. A strong
¹⁹ intraseasonal cycle has implication on zooplankton sampling.

20 **1 Introduction**

21 **1.1 Background**

22 Zooplankton plays a vital role in food web of pelagic ecosystem by enabling the hierarchical trans-
23 port of organic matter from primary producers to higher trophic levels impacting the fish population
24 [Ohman and Hirche, 2001] and the carbon pump of the deep ocean [Le Qu et al., 2016]. They are
25 presumably the largest migrating organisms in terms of biomass [Hays, 2003] which occurs in diel
26 vertical migration (DVM). Zooplankton depend not only on phytoplankton but other environmental
27 parameters (e.g. mixed layer depth, insolation, oxygen, thermocline, nutrient availability, chloro-
28 phyll concentration and daily primary production). The biological productivity of the ocean is
29 essentially connected with physics and chemistry [Subrahmanyam, 1959, Ryther et al., 1966, Qasim,
30 1977, Nair, 1970, Banse, 1995, McCreary et al., 2009, Vijith et al., 2016, Amol et al., 2020]. The
31 dynamic ocean results in varying physico-chemical properties, leading to bloom and growth of
32 plankton in favourable conditions. The changes are strongly influenced by the seasonal cycle in the
33 North Indian Ocean (NIO; north of 5 °N of Indian Ocean). The eastern boundary of Arabian Sea
34 contains the West India Coastal Current ([Ramamirtham and Murty, 1965, Banse, 1968, Shetye
35 et al., 1990, McCreary Jr et al., 1993, Amol et al., 2014, Vijith et al., 2016, Chaudhuri et al., 2020,
36 WICC]) which reverses seasonally, flowing poleward (equatorward) during November to February
37 (June to September).

38 A direct consequence of this reversal is the seasonal cycle of thermocline, oxycline and thickness
39 of mixed Layer Depth (MLD) induced by upwelling (downwelling) favourable conditions in summer
40 (winter) eastern Arabian Sea (EAS) facilitated further by wind speed and near-surface stratifica-
41 tion. Further, the phytoplankton biomass and chlorophyll concentration changes with the season

42 [Subrahmanyam and Sarma, 1960, Banse, 1968, Lévy et al., 2007, Vijith et al., 2016]. Upwelling in
43 summer monsoon leads to maximum chlorophyll growth in the entire EAS [Banse, 1968, Banse and
44 English, 2000, McCreary et al., 2009, Hood et al., 2017, Shi and Wang, 2022]. During winter mon-
45 soon, the convective mixing induced winter mixed layer [Shetye et al., 1992, Madhupratap et al.,
46 1996b, McCreary Jr et al., 1996, Lévy et al., 2007, Shankar et al., 2016, Vijith et al., 2016, Keerthi
47 et al., 2017, Shi and Wang, 2022] results in winter chlorophyll peak in northern EAS (NEAS) while
48 the downwelling Rossby waves modulate chlorophyll along the southern EAS (SEAS) albeit limited
49 to coast and islands [Amol et al., 2020].

50 The zooplankton grazing peak is instantaneous with no time delay from peak phytoplankton
51 production [Li et al., 2000, Barber et al., 2001], but its population growth lags [Rehim and Imran,
52 2012, Almén and Tamelander, 2020] depending on its gestation period and other limiting aspects.
53 While some studies suggest that the peak timing of zooplankton may not change in parallel with
54 phytoplankton blooms [Winder and Schindler, 2004], others indicate that lag exists between primary
55 production and the transfer of energy to higher trophic levels [Brock and McClain, 1992, Brock
56 et al., 1991]. The conventional zooplankton measurements, where only few snapshot/s of the event
57 is captured gives an incoherent or incomplete understanding in terms of spatio-temporal variation
58 of zooplankton [Ramamurthy, 1965, Piontkovski et al., 1995, Madhupratap et al., 1992, 1996a,
59 Wishner et al., 1998, Kidwai and Amjad, 2000, Barber et al., 2001, Khandagale et al., 2022] as
60 much information is revealed by later studies [Jyothibabu et al., 2010, Vijith et al., 2016, Shankar
61 et al., 2019, Aparna et al., 2022] using high resolution data. Calibrated acoustic instruments such
62 as acoustic Doppler current profiler (ADCP) along with relevant data can be utilised to understand
63 small scale variability [Nair et al., 1999, Edvardsen et al., 2003, Smith and Madhupratap, 2005, Smeti
64 et al., 2015, Kang et al., 2024], the complex interplay between the physico-chemical parameters and

65 ecosystem [Jiang et al., 2007, Potiris et al., 2018, Shankar et al., 2019, Aparna et al., 2022, Nie
66 et al., 2023], the zooplankton migration [Inoue et al., 2016, Ursella et al., 2018, 2021] and their
67 seasonal to annual variation [Jiang et al., 2007, Hobbs et al., 2021, Liu et al., 2022, Aparna et al.,
68 2022].

69 The relationship between backscatter and the abundance and size of zooplankton was described
70 by Greenlaw [1979] wherein it was pointed out that single frequency backscatter can be used to esti-
71 mate abundance if mean zooplankton size is known. A drastic increase in study temporal and spatial
72 variation of zooplankton biomass using backscatter-proxy came in 1990s by introduction of high
73 frequency echo sounders, with studies [Flagg and Smith, 1989, Wiebe et al., 1990, Batchelder et al.,
74 1995, Greene et al., 1998, Rippeth and Simpson, 1998] methodically showing acoustic backscatter
75 estimated zooplankton biomass. Net sampling augmented ADCP backscatter have been used to
76 study DVM and the spatial and temporal variability of zooplankton biomass in different marine
77 regions, such as the Southwestern Pacific, the Lazarev Sea in Antarctica and the Corsica Channel
78 in the north-western Mediterranean Sea [Cisewski et al., 2010, Hamilton et al., 2013, Smeti et al.,
79 2015, Guerra et al., 2019]. The first such study to exploit the potential of ADCPs in EAS was
80 carried out by Aparna et al. [2022] (A22 from hereon) using ADCP moorings deployed on conti-
81 nental slopes off the Indian west coast. In their work, they showed that the zooplankton standing
82 stock (ZSS) in fact declines during upwelling facilitated increase in phytoplankton biomass. The
83 unusual interaction implies the break down of existing understanding of predator-prey relationship
84 in fundamental level of marine food chain.

85 **1.2 Objective and scope of the manuscript**

86 A network of ADCPs has been installed off the continental slope and shelf on the west coast of
87 India. This ADCPs have enabled a rigorous view of intraseasonal to seasonal scale variability [[Amol](#)
88 [et al., 2014](#), [Chaudhuri et al., 2020](#)] of WICC. In the recent study A22 have used ADCP moorings
89 off Mumbai, Goa and Kollam to explain the temporal variability of zooplankton biomass. The
90 study showed that the zooplankton peaks (and troughs) is not only non-uniform in latitude but
91 also heavily influenced by the oxygen minimum zone, MLD and the seasonal upwelling/downwelling
92 conditions. Stark contrast in the phytoplankton bloom and subsequence growth of zooplankton or
93 the lack thereof was observed in the EAS regimes.

94 We extend the work of A22 by presenting data from four additional moorings in the EAS, show-
95 casing the deviations of seasonal cycle from climatology, and discussing the significant intraseasonal
96 variability of biomass and standing stock revealed by the ADCP data. The paper is organized as
97 follows; datasets and methods employed are described in section 2. Section 3 describes the observed
98 climatology of zooplankton biomass and standing stock. A comparison is drawn to the results of
99 A22. Further, the seasonal cycle of zooplankton biomass and standing stock is discussed with re-
100 lation to the MLD, oxygen, temperature and circulation in determining the biomass is discussed
101 in results section 4. Section 5 delves deeper into the intraseasonal variability with summary and
102 conclusion in section 6.

103 **2 Data and methods**

104 The backscatter data from ADCP and the zooplankton samples collected from the periphery of
105 mooring is described in this section. The backscatter derived from the echo intensity of the seven

¹⁰⁶ ADCP mooring deployed on the continental slope off the Indian west coast is the primary data
¹⁰⁷ we have use in this manuscript. The moorings details are summarized in [Table 1](#). In situ biomass
¹⁰⁸ data from volumetric zooplankton samples are used to validate and correlate with backscatter. The
¹⁰⁹ chlorophyll data is used to study and draw inferences for the possible zooplankton growth seasons.
¹¹⁰ In addition, we have used the monthly climatology of temperature and salinity from [Chatterjee](#)
¹¹¹ [et al.](#) [2012].

¹¹² 2.1 ADCP data and backscatter estimation

¹¹³ The ADCPs were deployed on the continental slope off the Indian west coast ([Fig. 1](#)), off Mumbai,
¹¹⁴ Goa, Kollam and Kanyakumari, and later extended to three more sites to cover the entire EAS
¹¹⁵ basin from Okha (22.26°N) in north to Kanyakumari (6.96°N) in south. The other two ADCPs
¹¹⁶ are, 1) Jaigarh at central EAS (CEAS) to NEAS transition zone (inclined towards CEAS), 2)
¹¹⁷ Udupi (primarily at SEAS regime) in the transition zone between CEAS and SEAS. The extended
¹¹⁸ moorings were deployed in October 2017, though Kanyakumari had been deployed earlier too.
¹¹⁹ However, only Mumbai, Goa and Kollam were part of the previous backscatter study by A22.
¹²⁰ The moorings are serviced on yearly basis usually during October–November or sometime during
¹²¹ September–December (depending on ship availability). The ADCPs are of RD Instruments make,
¹²² upward-looking and operate at 153.3 kHz. While utmost care is taken to position the instrument
¹²³ at ~ 200 m depth, yet for some deployments it's shallow or deeper owing to drift caused by floater
¹²⁴ buoyancy-anchor weight balance. Data was collected at hourly interval and the bin size was set to
¹²⁵ 4 m. The echoes at surface to 10% range (~ 20 m) means the data at these depths is rendered
¹²⁶ useless and is discarded from further use. We have followed the methodology laid down in A22 to
¹²⁷ derive the backscatter time series from ADCP echo intensity data. The gaps up to two days are

¹²⁸ filled using the grafting method of Mukhopadhyay et al. [2017] once the zooplankton biomass time
¹²⁹ series is constructed.

¹³⁰ 2.2 Zooplankton data and estimation of biomass

¹³¹ The zooplankton samples were collected in the vicinity (~ 10 km) of ADCP mooring site twice, once
¹³² prior retrieval and again post deployment of moorings so that there is overlap in the ADCP time
¹³³ instance and in situ zooplankton samples. The sampling is done at the mooring location during
¹³⁴ servicing cruises on board RV Sindhu Sankalp and RV Sindhu Sadhana (Table 2). Multi-plankton
¹³⁵ net (MPN) (100 μm mesh size, 0.5 m^2 mouth area) was used to get samples in the pre-determined
¹³⁶ depth ranges; water volume filtered was calculated by the product of sampling depth range and
¹³⁷ the mouth area of net. The depth range and timing of sample collection was different throughout
¹³⁸ the MPN hauls (refer Table 2). From 2020 onward, the depth-range was standardized to the bins
¹³⁹ of 0–25, 25–50, 50–75, 75–100, 100–150 (units are in meters). The backscatter obtained earlier
¹⁴⁰ is averaged in vertical corresponding to the specific MPN hauls for each site. The backscatter is
¹⁴¹ linear regressed with respective biomass to establish their relationship (Fig. 2), which has been
¹⁴² demonstrated in numerous previous studies [Flagg and Smith, 1989, Heywood et al., 1991, Jiang
¹⁴³ et al., 2007, Aparna et al., 2022].

¹⁴⁴ 2.2.1 Biomass time series and estimation of standing stock

¹⁴⁵ The zooplankton biomass time series (Fig. 3) is created from the above derived linear relationship.
¹⁴⁶ The standing stock is determined by taking the depth integral of biomass over the water column.
¹⁴⁷ To maintain the consistency of standing stock estimation, only those deployments that doesn't lack
¹⁴⁸ data at any depth in the entire range of 24–120 m are considered for analysis as in A22. The lack of

149 data in the above mentioned depth range is due to deviation in positioning of ADCP sensor in the
150 water column. A swift alteration in bathymetry along the continental slope implies that the mooring
151 might anchor at a different depth than planned, hence a change in the predicted position of ADCP.
152 This leads to gap in data at few mooring sites for some year. For example, for the northern-most
153 mooring at Okha, data is not available for the entire upper 120 m depth for the second deployment.
154 Also at Jaigarh, where the surface to \sim 60m data (in 3rd deployment) and Kollam, where 80 m
155 and below (in 4th deployment) is unavailable and hence discarded from standing stock estimation.
156 There are few deployments where no or bad data was recorded e.g, at Udupi (4th deployment) and
157 Kanyakumari (6th deployment).

158 **2.3 Mixed-layer depth, temperature, oxygen and chlorophyll**

159 As we are using a 153.3 kHz ADCP moored at \sim 150 m, the top \sim 10% of data is unusable because
160 of surface echoes. MLD in EAS is of the order \sim 20 to 40 m during summer monsoon [[Shetye et al., 1990](#), [Shankar et al., 2005](#), [Sreenivas et al., 2008](#)] especially in the SEAS [[Shenoi et al., 2005](#)],
161 but during winter the MLD in northern NEAS remains deep [[Shankar et al., 2016](#)]. Although it
162 is possible to use the near-surface ADCP data after due noise correction, it is beyond the scope of
163 present study. The temperature data is used from [Chatterjee et al. \[2012\]](#), a monthly climatology
164 having 1° spatial resolution. Monthly climatology of oxygen data is obtained from World Ocean
165 Atlas 2013 [[García et al., 2014](#)] which contains objectively analyzed 1° climatological fields of in
166 situ measurements. Previous study based on ADCP data of EAS A22 have used SeaWiFS based
167 chlorophyll data for comparison with climatology of ZSS. The SeaWiFS was at its end of service
168 in 2010, hence we use new chlorophyll product from Global Ocean Colour, biogeochemical L3 data
169 obtained from [E.U. Copernicus Marine Service Information](#). The daily data is available at a spatial
170

₁₇₁ resolution of 4 km.

₁₇₂ 3 Time series and climatology

₁₇₃ The high and low productive biomass regime in upper and deeper depths is demarcated using a
₁₇₄ biomass contour as in A22 wherein they chose 215 mg m^{-3} as such, and it's depth is labeled as
₁₇₅ D215. However, in the present scenario we've moorings deployed at farther ends of EAS, namely
₁₇₆ Kanyakumari and Okha. The choice of biomass contour isn't abrupt; first, it is carefully chosen to
₁₇₇ accommodate the seasonal variation, as a shift to biomass contour lower than the z215 would be
₁₇₈ unviable as our data is only till 140 m depth. For example in the case of Kollam, the D215 exceeds
₁₇₉ 140 during few months of 2022 ([Fig. 3](#)). A higher biomass contour would lead to subdued view of
₁₈₀ the seasonal cycle as in the case of Kanyakumari and Okha where 215 mg m^{-3} biomass contour
₁₈₁ is often low enough to reach $\sim 20\text{--}30$ m depths ([Fig. 3](#)), hence z175 is chosen here. Second, it
₁₈₂ allows us to link the seasonal variation of biomass to the physico-chemical properties. Climatology
₁₈₃ of zooplankton biomass and ZSS is discussed at locations northward starting from southernmost
₁₈₄ mooring site i.e, Kanyakumari. The monthly climatology of biomass and ZSS is computed for
₁₈₅ all locations having valid data in 24–140 m depth range. Time series (climatology) of biomass is
₁₈₆ discussed in the following ([subsection 3.2](#)) section.

₁₈₇ 3.1 Time series description

₁₈₈ A preliminary analysis of the biomass time series in daily and monthly averaged scale shows that
₁₈₉ the biomass decreases with increasing depth ([Fig. 3](#)) at all the seven locations. Rate of biomass
₁₉₀ decrease with depth, roughly defined as the difference between mean biomass at 40 m and 104 m
₁₉₁ depth is highest off Jaigarh and Mumbai as it has higher biomass in upper ocean ([Fig. 4 c,b](#)) and

lowest off Kanyakumari. This is followed by CEAS locations Goa and Udupi (Fig. 4 d,e). While the biomass decrease with depth is lower off Kollam from 2017 to 2020, it becomes considerably high from thereon (Fig. 4 f). A comparatively weaker decline in zooplankton biomass with respect to depth off Okha (Fig. 3 a1,a2) at NEAS is agreeing with earlier reported data [Wishner et al., 1998, Madhupratap et al., 2001, Smith and Madhupratap, 2005, Jyothibabu et al., 2010]. The sites at SEAS, especially off Kanyakumari and 2017 to 2020 off Kollam also have weaker decrease [Madhupratap et al., 2001, Jyothibabu et al., 2010, Aparna et al., 2022]. However, the biomass decline with depth post 2020 off Kollam is high owing to a strong bloom in these years and is reflected as D215 deepening. D175 and D215 is deep throughout EAS during winter monsoon, but the occurrence of high biomass is distinct to each regime of EAS. Upper ocean shows considerably high biomass and ZSS during winter monsoon at NEAS. On the contrary at SEAS, the upper ocean shows higher biomass during summer monsoon even though the D215 and D175 is shallower during this period.

The mean, standard deviation of biomass, ZSS and chlorophyll are shown in Table 3. A pattern develops from analysis of mean and standard deviation of biomass at 40 and 104 m, with comparatively lower mean biomass off Okha and Goa bifurcated by higher mean biomass off Mumbai and Jaigarh. Similarly, the lower mean biomass off Udupi and Kanyakumari is divided by higher mean biomass off Kollam. The sites with higher biomass tends to have higher variation over time e.g. Mumbai, Jaigarh and Kollam. Variation in the monthly average or seasonal cycle over time suggests significant interannual variability.

212 **3.2 Climatology of zooplankton biomass and standing stock**

213 **3.2.1 Southern EAS**

214 During mid-March off Kanyakumari, the depth of 23°C isotherm (henceforth D23) shallows along-
215 with oxycline (marked by 2.1 ml L^{-1} , a higher oxygen contour as it lies outside OMZ core) and a
216 rise in biomass is observed ([Fig. 5 g1](#)). The z175 is shallower from May onward to October and the
217 zooplankton biomass is comparatively higher than rest of the year. From October z175 starts to
218 deepen and the relatively high biomass in water column is maintained till late December. However,
219 the deepening of D175 isn't reflected as an increase in ZSS because of low biomass in the entire
220 water column. A gradual increase is seen in the chlorophyll biomass starting from April and the
221 peak is attained in June ([Fig. 5 g2](#)). The ZSS is increased in June, however the growth is minimal.
222 There is almost no seasonal variation in ZSS off Kanyakumari ($2.02\text{ gm m}^{-2} 3\sigma$ of ZSS) as compared
223 to the chlorophyll variation ($1.53\text{ mg m}^{-3} 3\sigma$ of Chl).

224 At the nearest northern mooring site off Kollam (ZSS standard deviation, 3.75 gm m^{-2}) a
225 strong seasonal cycle is observed and the D215 is deeper for any given month. A higher biomass
226 is present in the larger portion of water column and the D215 is at $\sim 110\text{ m}$ during Mar–May
227 ([Fig. 5 f1](#)). Starting from March, the D215 begins to shallow with progress in time till August.
228 During this period, a sharp decrease is seen in the D23 ($\sim 80\text{ m}$ in June to September) while the
229 oxycline (1.7 ml L^{-1} overshoots and reaches $\sim 40\text{ m}$ ([Fig. 5 f1](#)). A decline (steep-rise) in ZSS
230 (chlorophyll biomass) is seen off Kollam and its minimum (peak) is attained in August ([Fig. 5 f2](#)).
231 The chlorophyll biomass decreases rapidly in the following months, while the ZSS increases and a
232 maximum is seen during October. This feature was previously reported by A22, highlighting an
233 imbalance in the interaction between zooplankton and phytoplankton.

234 A similar feature is seen further north, off Udupi which sits at the transition zone of SEAS and

²³⁵ CEAS, albeit with a relatively weaker zooplankton biomass. The peak of chlorophyll and minimum
²³⁶ of ZSS occurs in September ([Fig. 5 e2](#)) which is one month later than off Kollam. The 2.1 ml L^{-1}
²³⁷ oxygen contour reaches to a much shallow depth of $\sim 20 \text{ m}$ during July to October unlike any
²³⁸ other location in EAS due to strong upwelling. The D215 vaguely follows D23; with the gradual
²³⁹ shallowing from March onward reaching $\sim 60 \text{ m}$ in September and a steep decline afterwards till
²⁴⁰ November ([Fig. 5 e1](#)).

²⁴¹ **3.2.2 Central EAS**

²⁴² The D215 seasonal trend off Goa in present study is similar to trend of D215 off Goa as described
²⁴³ in A22. It is also analogous to D215 trend off Udupi since they are entirely restricted by D23 and
²⁴⁴ 1.7 ml L^{-1} oxygen contour that closely follows it. Although we witness an increase in chlorophyll
²⁴⁵ biomass during October, the D215 is restricted to the $\sim 50 \text{ m}$ in this period and the ZSS is at
²⁴⁶ minimum similar to off Udupi (Kollam) during September (August). The ZSS rapidly increases
²⁴⁷ and reaches its maximum in January, sustained till March and then gradually declines. Unlike the
²⁴⁸ previous locations, the biomass off Goa decreases rapidly below the z215 as reported earlier in A22,
²⁴⁹ reaching as low as 60 mg m^{-3} at 130 m during June to September ([Fig. 5 d1](#)).

²⁵⁰ The ZSS off Jaigarh is identical but stronger to that of off Goa, owing to higher biomass above
²⁵¹ z215 and the comparatively deeper D215 ([Fig. 5 c1](#)). From the ZSS maximum in February ([Fig. 5](#)
²⁵² c2), it steadily decreases and attains a minimum in September, a rapid rise is seen in the following
²⁵³ months. What's intriguing is a presence of strong variation in ZSS off Jaigarh (3σ is 9.72 gm m^{-2} ,
²⁵⁴ highest among all locations) although the seasonal variation in chlorophyll biomass ([Fig. 5 c2](#)) is
²⁵⁵ visibly non-existent ($0.15 \text{ mg m}^{-3} 3\sigma$ of Chl) and lowest among all locations. This is an exact
²⁵⁶ opposite scenario of Kanyakumari, where an insignificant seasonal variation in ZSS is seen even

257 though the chlorophyll biomass varies strongly.

258 Starting from Kollam ([Fig. 5 f1](#)) and moving northward to Jaigarh ([Fig. 5 c1](#)), we see that the
259 core of high zooplankton biomass gradually shifts from summer (off Kollam) to winter monsoon
260 (off Jaigarh), with the transition of upper ocean zooplankton biomass happening along Udupi and
261 Goa. On the contrary, chlorophyll biomass tends to have low seasonal range as we move northward
262 from SEAS, with Jaigarh having the least seasonal variation. This shift along with winter monsoon
263 facilitated deeper thermocline leads to an even larger impact on ZSS.

264 **3.2.3 Northern EAS**

265 Further north off Mumbai the D215 is deeper in December to early April, resulting in a higher
266 ZSS ([Fig. 5 b2](#)). D23 follows D215 and the oxycline follows an erratic pattern, reaching depths
267 > 140 m during January to March ([Fig. 5 b1](#)); when a higher biomass is observed above z215.
268 The chlorophyll biomass shows seasonal variation albeit lower than the SEAS counterpart. The
269 ZSS increases rapidly from its minima in October in the following month as the D215 deepens and
270 the maximum occurs in February. The chlorophyll biomass decreases from March and a gradual
271 decrease in ZSS is seen till July, after which the ZSS basically flattens even though the chlorophyll
272 increases.

273 At the northernmost site of EAS i.e, off Okha, a noticeable feature is a much higher oxygen in
274 upper ocean except during summer monsoon, therefore a higher oxygen contour (3.2 ml L^{-1}) is
275 used for the oxycline contour. Biomass above z175 is much weaker ([Fig. 5 a1](#)) leading to a relatively
276 lower ZSS ([Fig. 5 a2](#)) compared to Mumbai. The D175 shallows from February to it's minimum in
277 August. There's two chlorophyll peak off Okha, one in February due to convective mixing induced
278 deepening of MLD [[Wiggert et al., 2005](#), [Lévy et al., 2007](#), [Keerthi et al., 2017](#), [Shankar et al., 2016](#)]

279 and the other during August in summer monsoon [Wiggert et al., 2005, Lévy et al., 2007]. The ZSS
280 remains flat in summer monsoon period i.e, June to September, although the chlorophyll biomass
281 increases in this time. Afterwards, ZSS gradually increases and attains its maximum in February
282 same as the chlorophyll biomass. ZSS sustains this maximum till March, declines rapidly in April
283 and then gradually till July.

284 4 Seasonal cycle and variability

285 This section will deal with a discussion on the seasonal cycle and variability of biomass and ZSS in
286 annual and intra-annual scale along the three regimes of EAS.

287 To understand the variation at a specific period, say 365-days (annual cycle) or 180-days (semi-
288 annual cycle), wavelet analysis is carried out for biomass ([Fig. 6](#)) and ZSS ([Fig. 7](#)). However, if
289 we wish to understand the variation in a specific period band, we use Lanczos filtered zooplankton
290 biomass. It is digital analogous to physical filters used in biology labs to filter all zooplankton
291 within a size range. The former technique gives us an idea about variation of biomass occurring
292 with time at all period while the later shows variation of biomass within a period band of interest.
293 Incorrect placement of ADCP or instrument issues may lead to gaps in time series data, e.g., Okha's
294 second deployment (2019–2020) lacked data for the top 140 meters because of deeper than intended
295 placement depth. The gaps in time series makes it hard to analyze annual cycles in regions with
296 limited data. Therefore, we consider locations other than Okha and Jaigarh for the 40 m biomass
297 and ZSS in annual scale.

298 The biomass time series is decomposed into distinct period bands spanning days to months.
299 Among these DVM is the simplest variation, determining zooplankton biomass at a given depth with
300 higher (lower) biomass at night (day). On a longer time scale, annual variability reflects changes over

the course of a year often influenced by seasonal cycles like monsoons. For example, in the case of phytoplankton, upwelling favored by monsoonal winds can vary from year-to-year, thus determining the biomass for a given year uniquely. Intra-annual variability captures fluctuations that occur between seasons, shorter than a year but longer than a season, e.g., while both summer and winter monsoons are the growing season for chlorophyll at NEAS, the strength of bloom varies with season. Intraseasonal variability is about shifts occurring within a season, typically lasting weeks to months and driven by short-term environmental changes, e.g., nutrient replenishment (depletion) in short-span due to upwelling and/or entrainment (bloom). The strength and contribution of variability components changes over time and differs between EAS regimes. For instance, in 2019 off Kollam (Fig. 8), intraseasonal variability was dominated by it's high-frequency components (period $<\sim 30$ days). An increase in biomass during the summer monsoon was due to low-frequency component of seasonal cycle, i.e., intra-annual and annual variability. However, a sharp decline in August resulted from reduced intra-annual and intraseasonal variability, even with the presence of a weakly positive annual variability.

From the linear equation correlating biomass and backscatter, the upper and lower bound of error limits equals to $\sim 14 \text{ mg m}^{-3}$ (Fig. 2). The standard deviation incorporating 99.73 % data i.e., $\pm 3 * \sigma$ of annual variability results in its range of 40 mg m^{-3} . The intra-annual variability has a range of 80 mg m^{-3} . This higher range of variability compared to the error range permits us to infer information reliably.

4.1 Annual cycle and annual variability

The annual cycle of biomass off Kanyakumari (Udupi and Kollam) is weak (strong), but it varies in time. For example off Kollam, the wavelet power is stronger post 2020 (Fig. 6 f). The biomass

323 over 24–120 m of water column is integrated to obtain the ZSS time series. The absence (presence)
324 of ZSS annual cycle off Kanyakumari (off Udupi) is confirmed with wavelet analysis ([Fig. 7 g1](#)). To
325 capture the annual variability, the biomass is passed through Lanczos filter within period of 300 to
326 400 days ([Fig. 9](#)). The annual variability off Kanyakumari (22 mg m^{-3}) is least among all mooring
327 sites, but Kollam shows strong annual variability implying the year-to-year variation of biomass is
328 significant.

329 Off Goa, the annual cycle of biomass is comparatively weak contrary to the results of A22, owing
330 to shorter time record and low biomass in the recent years as reflected in its ZSS wavelet for 2018
331 to early 2020 (2021 and 2022) ([Fig. 7 d1](#)) resulting in a weak (strong) annual variability ([Fig. 10](#))
332 and is also seen components of biomass variability ([Fig. 8](#)). An interesting feature is observed at
333 the core of annual filtered biomass lying at 50 m, which seems similar to the core of annual filtered
334 along-shore current from [Nethery and Shankar \[2007\]](#). This alone, however, cannot be used as
335 evidence for causation of relation.

336 Further north, a strong annual cycle dominates the seasonal cycle of biomass (40 m and 104 m
337 [Fig. 6](#)) agreeing with A22. The annual variability is strong off Mumbai and Jaigarh with 3σ range
338 of 41 and 54 mg m^{-3} , respectively, which is highest among EAS regimes. Biomass variability in
339 annual scale decreases minutely with depth off Mumbai and the three CEAS sites than off Kollam
340 ([Fig. 9](#)) similar to the observed ocean currents [[Chaudhuri et al., 2020, 2021](#)]. The annual cycle and
341 annual variability of biomass and subsequently, ZSS increases along the slope as we go northward
342 to Mumbai from Kanyakumari.

343 **4.2 Semi-annual cycle and intra-annual variability**

344 Along with the annual cycle we observe presence of semi-annual cycle at most locations and together
345 they constitute the seasonal cycle. The variability at intra-annual band ([Fig. 10](#)) tends to be
346 stronger compared to the annual variability. Much like the annual cycle, the semi-annual cycle and
347 intra-annual variability is weak off Kanyakumari compared to Kollam and Udupi. However, the
348 strong variability in intra-annual scale is restricted to upper ocean for few years off Kollam such as
349 during 2018, 2021 and 2022. Similar to WICC variability, the intra-annual component dominates
350 the seasonal cycle and is strong off Kollam [[Chaudhuri et al., 2020](#)].

351 Off Goa and Jaigarh, the semi-annual cycle tends to be strong, specifically during 2022 when a
352 anomalous bloom is observed throughout EAS. The semi-annual cycle weakens with depth ([Fig. 6](#),
353 d) in these locations. Intra-annual component of seasonal cycle is observed off Goa, with weak
354 (strong) variability during 2019 (2020, 2022) ([Fig. 10](#), d) and is moderately strong off Jaigarh.
355 Spread of energy among all intra-annual periods for 2022 ([Fig. 6](#)) off Goa, while during 2019 and
356 2020 the wavelet energy is only present in the semi-annual periods resulting in a overall weaker
357 intra-annual component ([Fig. 8](#)).

358 The intra-annual band's strength is reduced off Mumbai and Okha as compared to CEAS and
359 SEAS. The semi-annual cycle is moderately present at 40 m ([Fig. 6](#)) off Mumbai which weakens at
360 104 m ([Fig. 6](#)) resulting in annual cycle dominated ZSS. Analysis reveals the presence of moderately
361 strong semi-annual cycle off Okha only at 104 m and it's intra-annual (annual) band is similar
362 (weaker) in magnitude as compared to Mumbai. Excluding Kanyakumari, intra-annual variability
363 of biomass decreases poleward with higher variation seen off Kollam, Udupi and Goa similar to the
364 ocean currents [[Amol et al., 2014](#), [Chaudhuri et al., 2020, 2021](#)].

³⁶⁵ 5 Intraseasonal variability

³⁶⁶ The intraseasonal band defined as the variability occurring between periods of few days to 90 days is
³⁶⁷ split into two categories; a high-frequency (period < 30 days) and a low-frequency (30 < period < 90
³⁶⁸ days) component. The presence of significant variation in the 30-day running mean with recurring
³⁶⁹ bursts are seen in the daily data and in the wavelet analysis of biomass at 40 m and 104 m ([Fig. 6](#))
³⁷⁰ as bursts during few days to a week distinctive to each mooring location. Most of these bursts are
³⁷¹ occurring due to the high-frequency component of intraseasonal band of biomass. Our primary focus
³⁷² is in the low-frequency component of intraseasonal variability (henceforth, intraseasonal variability)
³⁷³ i.e, within 30–90 days. The intra-seasonal component is transient in nature and its magnitude is
³⁷⁴ higher than the other two low-frequency variabilities discussed in [section 4](#). With a $3^*\sigma$ range of
³⁷⁵ 80 mg m^{-3} for variability in this band, we can obtain significant inferences.

³⁷⁶ Off Kanyakumari the intraseasonal variability is much strong unlike the variability in it's annual
³⁷⁷ and intra-annual bands. This, along-with the wavelet at 40 and 104 m suggests that the short-
³⁷⁸ term environmental changes drives the biomass off Kanyakumari which is also reflected in the ZSS
³⁷⁹ ([Fig. 7 g2](#)). Off Kollam and Udupi, the intraseasonal bursts are significant but due to an equal role
³⁸⁰ of intra-annual component the biomass isn't solely driven by short-term environmental changes.
³⁸¹ Strong variability in intraseasonal scale seems to occur during August to November, for example
³⁸² off Kanyakumari(2018, 2019 and 2020), off Kollam (2018, 2021 and 2022) and off Udupi (2018)
³⁸³ although it can extend to mid-summer/mid-winter monsoon for few years.

³⁸⁴ Off Goa, significant peaks in wavelet spectra in intraseasonal band is present in biomass ([Fig. 6](#),
³⁸⁵ d1, d2) and ZSS ([Fig. 7,d1](#)). During 2019, the intra-annual variability off Goa is non-existent
³⁸⁶ and with the weak annual variability, a rather constant ZSS is observed ([Fig. 7, d2](#)) and also 40
³⁸⁷ m biomass ([Fig. 8](#)). But ZSS varies briefly during September–November of 2019 as seen by the

388 presence of spectra intraseasonal band ([Fig. 7](#), d1). It occurred strongly in 2018 ([Fig. 11](#)) and later
389 in 2020 during same transition monsoon, but the absence intra-annual band in 2019 makes it easier
390 to comprehend the contribution of intraseasonal variability. A similar feature is noted off Jaigarh
391 albeit with a weaker magnitude.

392 Weak presence of intraseasonal variability ([Fig. 11](#)) is also noted in the relatively smoother
393 30-day rolling mean ZSS off Mumbai ([Fig. 7](#), b2) and Okha ([Fig. 7](#), a2). Although spectra in the
394 intraseasonal band is present at 40 m off Mumbai and Okha (b2, b1 of [Fig. 6](#)), it is almost absent
395 at 104 m except for a select few years. For example, during early 2021 off Mumbai, the presence
396 of strong intraseasonal peaks in wavelet spectra of 104 m ([Fig. 6](#) b2) along with 40 m ([Fig. 6](#)
397 b1) shows up in the ZSS spectra ([Fig. 7](#) b1) and also in the biomass variability in intraseasonal
398 scale ([Fig. 11](#)). It implies that the variability can be restricted to upper ocean. Off Okha, the
399 intraseasonal variability is lowest among all EAS sites with 3σ range of 64 mg m^{-3} followed by
400 Mumbai. However, Okha has weak annual and intra-annual variability unlike Mumbai leading to
401 least predictability.

402 The wavelet power at different depth shows peaks in low-frequency intraseasonal band across
403 EAS. Compared to 40 m, wavelet power at 104 m suggests a decrease in its strength at respective
404 locations most often. The intraseasonal peaks in ZSS are strong in SEAS followed by CEAS and
405 is weak off NEAS sites. Lanczos filtered biomass shows that the intraseasonal variability is strong
406 during August to November off all location and is coherent in many instances along much of the EAS
407 slope as seen during 2018 ([Fig. 11](#)). The strength of intraseasonal variability of biomass is in contrast
408 to the WICC intraseasonal band which is strong during winter monsoon at slope [[Amol et al.,](#)
409 [2014](#), [Chaudhuri et al., 2020](#)] and shelf [[Chaudhuri et al., 2021](#)]. Yet the magnitude of intraseasonal
410 variability of biomass decreases as we move poleward much like the observed intraseasonal currents.

411 **6 Discussion**

412 **6.1 Summary**

413 The zooplankton biomass and standing stock across different regions of EAS was examined in this
414 article, highlighting their spatio-temporal trends in the light of physico-chemical parameters using
415 the multi-yearlong ADCP backscatter data from 2017 to 2023.

416 The findings shows notable seasonal variation in zooplankton biomass and ZSS; In SEAS the
417 higher biomass is observed during summer monsoon, while in NEAS the high biomass is observed
418 during winter monsoon with transition of peak biomass happening gradually along CEAS regime
419 ([subsection 3.2](#)). Off Kollam, a unique double peak in ZSS occurs, one during May to July and
420 another in September to November, suggesting a complex interplay between environmental drivers
421 and zooplankton growth ([Fig. 5 f2](#)). Off Kanyakumari, the seasonal variation in ZSS is non-existent
422 even though a dramatic seasonality is seen in primary production. Climatology shows strong decline
423 in biomass w.r.t. depth off Goa, then NEAS sites off Jaigarh, Mumbai and Okha followed by SEAS
424 locations off Udupi, Kollam and Kanyakumari.

425 Seasonal cycle and variability play a crucial role in regulating biomass. A strong annual cycle is
426 observed in Northern sites like Mumbai and Jaigarh ([Fig. 6](#)), with biomass peaking during winter
427 monsoon months ([Fig. 5](#)). However, the Southern and Central regions particularly off Kollam,
428 exhibit more complex patterns. Off Kollam, the presence of a weak annual cycle and a stronger
429 semi-annual cycle is noted along with a moderately strong biennial cycle. The semi-annual cycle is
430 especially prominent in the Southern EAS ([subsection 4.2](#)), where it contributes significantly to the
431 seasonal biomass changes, while northern regions is dominated by annual cycle ([subsection 4.1](#)).

432 Intraseasonal variability is found to influence zooplankton biomass significantly, especially in

433 the summer to winter monsoon transition months ([Fig. 11](#)), while the high frequency (period <
434 ~ 30 days) variability determine changes in smaller temporal scale ([Fig. 8](#)) as seen in the daily
435 biomass record. Intraseasonal variability is higher in the Southern EAS, with the Northern regions
436 displaying less variance. The variability in annual scale is weak, while that in intra-annual scale
437 is often comparable to intraseasonal variability. Investigating the similarity of biomass variability
438 with current variability within respective bands shows that signs of currents influence on biomass
439 but establishing the connection requires further analysis.

440 **6.2 consequences of intraseasonal variability**

441 However, it is evident that the high-frequency intraseasonal variability dominates the zooplankton
442 biomass along EAS regime ([section 5](#)). A strong intraseasonal component suggests huge implications
443 on sampling, predictability and zooplankton patchiness.

444 **6.2.1 Implication on sampling**

445 The intra-seasonal component is transient and its magnitude is higher than the low frequency
446 variabilities ([Fig. 8](#)). In NEAS for example, the SST induced fronts that lasts one to two week
447 ([[Sarma et al., 2018](#), [Sarkar et al., 2019](#)]) can make the region more productive than the surrounding
448 ocean with an increase in integrated Chlorophyll-a ([\[Sarma et al., 2018\]](#)). This could be leading
449 to the spikes in biomass that is observed in the low-period (< 30 days) intraseasonal variability
450 as seen off Mumbai Goa and Kollam ([Fig. 8](#)). Strong dependency of zooplankton biomass on the
451 intra-seasonal variation has implication on the sampling of zooplankton using cruises. A servicing
452 cruise along the EAS moorings takes about 12 to 15 days excluding the time to and fro from port
453 to first/last mooring [[Chaudhuri et al., 2020](#), [Aparna et al., 2022](#)]. However, a sampling cruise

454 dedicated to study the spatial variation of zooplankton [Madhupratap et al., 1992, Smith et al.,
455 1998, Wishner et al., 1998, Kidwai and Amjad, 2000], say for summer monsoon may last a month or
456 more with coarse sampling interval and hence fail to capture the actual biomass within a season for
457 a fair spatial comparison. One such occasion is a dip in zooplankton biomass off Kollam because of
458 intraseasonal variability during August, 2019 (Fig. 8). The resulting biomass is low even though the
459 primary production in SEAS [Asha Devi et al., 2010, Jyothibabu et al., 2010] is high and subsequent
460 zooplankton biomass is supposed to be high.

461 **6.2.2 Zooplankton patchiness**

462 The species distribution of phytoplankton and further zooplankton in EAS is determined by intricate
463 play based on predation, environment, competition [Raghukumar and Anil, 2003] and hence the
464 forms change [Madhupratap et al., 1996a, Kidwai and Amjad, 2000, Raghukumar and Anil, 2003,
465 Smith and Madhupratap, 2005, Khandagale et al., 2022], with few species dominating in certain
466 seasons. Habitat patchiness, i.e, irregular distribution of habitats and resources in the deep-sea
467 environment [Eggleson et al., 1998, Raghukumar and Anil, 2003] contributes to high biodiversity
468 which in turn can affect ecosystem dynamics. A high intraseasonal variability in zooplankton
469 biomass suggests that patchiness in the deep-sea environment isn't solely driven by seasonal cycles
470 but also occurs within individual seasons. Carefully planned sampling of zooplankton with low
471 intervals is necessary to access the zooplankton patchiness within a season.

472 **6.2.3 Predictability**

473 Though EAS shows a strong seasonal cycle of current, there are notable differences between regimes
474 of EAS. Kollam's seasonal cycle is marked by intense intraseasonal bursts making the shelf WICC
475 at Kollam highly unpredictable [Chaudhuri et al., 2021] and the intraseasonal variation decreases

equatorward. The direction of WICC at any given time of the year can be either poleward or equatorward owing to the bursts. Assuming that advection and entrainment can influence zooplankton forms and since the annual variation of biomass is much weaker, current driven intraseasonal variations of biomass in rather unpredictable manner is expected. The zooplankton biomass varies frequently and strongly within the season itself ([section 5](#)). This intraseasonal variability indicates that zooplankton populations and their patches fluctuate due to short-term changes, likely responding to factors like temperature shifts, food availability, or ocean environment. So, the current and zooplankton biomass both are dominated by intraseasonal variations much more than the annual cycle.

Finding similarity in the trend of increasing (decreasing) intraseasonal (annual) variability of biomass and currents as we go equatorward along the EAS slope is tempting, as it indicates a link between the two. In fact, the feature observed in annual filtered biomass off Goa is similar to the alongshore component ([subsection 4.1](#)), with the core of biomass and alongshore current lying at same depth for both. However, a rigorous study is necessary to indicate any such relationship. On similar note, the inter-annual variability of Chl-a is less in comparison to its seasonal variability [[Shi and Wang, 2022](#)] much like the zooplankton. Strong peaks in intraseasonal band in chlorophyll was evident in Lomb–Scargle periodogram (figure not shown), analogous to zooplankton biomass and ZSS, but lacked concrete evidence of direct correlation.

6.3 Conclusion

The results presented in this paper are based on the ADCP backscatter which is suitable for creating long-term time series of zooplankton biomass in open ocean. There are however, certain limitations to this approach. While the variation in depth is captured with in situ samples from

498 MPN, the variation in season is not adequately addressed owing to the limitation of months when
499 ADCP servicing cruises are undertaken. The west coast cruises for ADCP servicing are planned for
500 the monsoon transition months but may start as early as late September till December with few
501 exceptions such as 2022 when it was carried out in March. Since the intraseasonal and intra-annual
502 variability is almost double that of the annual one ([section 5](#)), the sampling done in particular
503 season for biomass-backscatter comparison isn't sufficient. For a better approach to capture the
504 seasonal variation, more in situ samples are needed from the less explored seasons.

505 While we are able to infer the biomass information, any information regarding the size distribu-
506 tion of zooplankton and their contribution to ZSS is lost. In western Arabian sea, microzooplank-
507 ton dominated the grazing processes by consuming approximately 71 % of the primary production
508 [[Reckermann and Veldhuis, 1997](#), [Marra and Barber, 2005](#), [Landry, 2009](#)]. Mesozooplankton, in
509 turn relied on microzooplankton for about 40 % of their food [[Landry, 2009](#), [Hood et al., 2024](#)].
510 However, the relative grazing importance of micro and mesozooplankton fluctuated seasonally and
511 spatially, affecting the overall impact on phytoplankton biomass in a way that aligns with the theory
512 of grazing control or trophic cascade [[Ripple et al., 2016](#)] in the Arabian Sea [[Marra and Barber,](#)
513 [2005](#), [Landry, 2009](#)]. To understand the intricate complexities of different forms of meso- and mi-
514 crozooplankton and their interaction, a robust multi-frequency, size-resolving backscatter data can
515 be utilised. However, a mono-frequency ADCP is more than enough to capture the intraseasonal
516 variation of zooplankton that will otherwise be left inaccessible by conventional sampling means.

517 7 Declaration of competing interest

518 The authors declare that they have no known competing financial interests or personal relationships
519 that could have appeared to influence the work reported in this paper.

520 **8 Acknowledgments**

521 The data were collected by xxx with fund provided under xxxx. The mooring programme is
522 supported by INCOIS (Indian National Centre for Ocean Information Services, Hyderabad) and
523 CSIR. We acknowledge the contribution of mooring division and ship cell of CSIR-NIO.

524 Ranjan Kumar Sahu expresses his acknowledgment to the Council of Scientific and Industrial
525 Research (CSIR) for sponsoring his fellowship. Additionally, he extends his thanks to Ashok
526 Kankonkar for providing the essential data, Rahul Khedekar for his data processing, Roshan D'Souza
527 for his diligent work in biological data analysis. Their contributions were invaluable to the successful
528 completion of this research.

529 **References**

- 530 Anna-Karin Almén and Tobias Tamelander. Temperature-related timing of the spring bloom and match between
531 phytoplankton and zooplankton. *Marine Biology Research*, 16(8-9):674–682, 2020.
- 532 P Amol, D Shankar, V Fernando, A Mukherjee, SG Aparna, R Fernandes, GS Michael, ST Khalap, NP Satelkar,
533 Y Agarvadekar, et al. Observed intraseasonal and seasonal variability of the west india coastal current on the
534 continental slope. *Journal of Earth System Science*, 123(5):1045–1074, 2014.
- 535 P Amol, Suchandan Bemal, D Shankar, V Jain, V Thushara, V Vijith, and PN Vinayachandran. Modulation of
536 chlorophyll concentration by downwelling rossby waves during the winter monsoon in the southeastern arabian
537 sea. *Progress in Oceanography*, 186:102365, 2020.
- 538 SG Aparna, DV Desai, D Shankar, AC Anil, Shrikant Dora, and R Khedekar. Seasonal cycle of zooplankton standing
539 stock inferred from adcp backscatter measurements in the eastern arabian sea. *Progress in Oceanography*, 203:
540 102766, 2022.
- 541 C.R. Asha Devi, R. Jyothibabu, P. Sabu, Josia Jacob, H. Habeebrehman, M.P. Prabhakaran, K.J. Jayalakshmi, and
542 C.T. Achuthankutty. Seasonal variations and trophic ecology of microzooplankton in the southeastern arabian
543 sea. *Continental Shelf Research*, 30(9):1070–1084, 2010. ISSN 0278-4343. doi: <https://doi.org/10.1016/j.csr.2010.02.007>. URL <https://www.sciencedirect.com/science/article/pii/S0278434310000439>.
- 545 K Banse and DC English. Geographical differences in seasonality of czcs-derived phytoplankton pigment in the
546 arabian sea for 1978–1986. *Deep Sea Research Part II: Topical Studies in Oceanography*, 47(7-8):1623–1677, 2000.

- 547 Karl Banse. Hydrography of the arabian sea shelf of india and pakistan and effects on demersal fishes. In *Deep sea*
548 *research and oceanographic Abstracts*, volume 15, pages 45–79. Elsevier, 1968.
- 549 Karl Banse. Zooplankton: pivotal role in the control of ocean production: I. biomass and production. *ICES Journal*
550 *of marine Science*, 52(3-4):265–277, 1995.
- 551 Richard T Barber, John Marra, Robert C Bidigare, Louis A Codispoti, David Halpern, Zackary Johnson, Mikel
552 Latasa, Ralf Goericke, and Sharon L Smith. Primary productivity and its regulation in the arabian sea during
553 1995. *Deep Sea Res. Part 2 Top. Stud. Oceanogr.*, 48(6-7):1127–1172, jan 2001.
- 554 H. P. Batchelder, J. R. VanKeuren, R. D. Vaillancourt, and E. Swift. Spatial and temporal distributions of acoustically
555 estimated zooplankton biomass near the marine light-mixed layers station ($59^{\circ}30'N$, $21^{\circ}00'W$) in the north atlantic
556 in may 1991. *Journal of Geophysical Research: Oceans*, 100:6549–6563, 1995. doi: 10.1029/94jc00981.
- 557 John C Brock and Charles R McClain. Interannual variability in phytoplankton blooms observed in the northwestern
558 arabian sea during the southwest monsoon. *Journal of Geophysical Research: Oceans*, 97(C1):733–750, 1992.
- 559 John C Brock, Charles R McClain, Mark E Luther, and William W Hay. The phytoplankton bloom in the north-
560 western arabian sea during the southwest monsoon of 1979. *Journal of Geophysical Research: Oceans*, 96(C11):
561 20623–20642, 1991.
- 562 Abhisek Chatterjee, D Shankar, SSC Shenoi, GV Reddy, GS Michael, M Ravichandran, VV Gopalkrishna,
563 EP Rama Rao, TVS Udaya Bhaskar, and VN Sanjeevan. A new atlas of temperature and salinity for the north
564 indian ocean. *Journal of Earth System Science*, 121:559–593, 2012.
- 565 Anya Chaudhuri, D Shankar, SG Aparna, P Amol, V Fernando, A Kankonkar, GS Michael, NP Satelkar, ST Khalap,
566 AP Tari, et al. Observed variability of the west india coastal current on the continental slope from 2009–2018.
567 *Journal of Earth System Science*, 129(1):57, 2020.
- 568 Anya Chaudhuri, P Amol, D Shankar, S Mukhopadhyay, SG Aparna, V Fernando, and A Kankonkar. Observed
569 variability of the west india coastal current on the continental shelf from 2010–2017. *Journal of Earth System
570 Science*, 130:1–21, 2021.
- 571 Boris Cisewski, Volker H Strass, Monika Rhein, and Sören Krägesky. Seasonal variation of diel vertical migration
572 of zooplankton from adcp backscatter time series data in the lazarev sea, antarctica. *Deep Sea Research Part I:
573 Oceanographic Research Papers*, 57(1):78–94, 2010.
- 574 Kent L Deines. Backscatter estimation using broadband acoustic doppler current profilers. In *Proceedings of the
575 IEEE Sixth Working Conference on Current Measurement (Cat. No. 99CH36331)*, pages 249–253. IEEE, 1999.
- 576 A Edvardsen, D Slagstad, KS Tande, and P Jaccard. Assessing zooplankton advection in the barents sea using
577 underway measurements and modelling. *Fisheries Oceanography*, 12(2):61–74, 2003.

- 578 David B Eggleston, Lisa L Etherington, and Ward E Elis. Organism response to habitat patchiness: species and
579 habitat-dependent recruitment of decapod crustaceans. *Journal of experimental marine biology and ecology*, 223
580 (1):111–132, 1998.
- 581 Charles N Flagg and Sharon L Smith. On the use of the acoustic doppler current profiler to measure zooplankton
582 abundance. *Deep Sea Research Part A. Oceanographic Research Papers*, 36(3):455–474, 1989.
- 583 H. E. García, R. A. Locarnini, T. P. Boyer, J. I. Antonov, A. V. Mishonov, O. K. Baranova, M. M. Zweng, J. R.
584 Reagan, and D. R. Johnson. Dissolved oxygen, apparent oxygen utilization, and oxygen saturation. *NOAA Atlas*
585 *NESDIS 75*, 3, 2014.
- 586 Charles H Greene, Peter H Wiebe, Chris Pelkie, Mark C Benfield, and Jacqueline M Popp. Three-dimensional
587 acoustic visualization of zooplankton patchiness. *Deep Sea Research Part II: Topical Studies in Oceanography*, 45
588 (7):1201–1217, 1998.
- 589 Charles F Greenlaw. Acoustical estimation of zooplankton populations 1. *Limnology and Oceanography*, 24(2):
590 226–242, 1979.
- 591 Davide Guerra, Katrin Schroeder, Mireno Borghini, Elisa Camatti, Marco Pansera, Anna Schroeder, Stefania
592 Sparnocchia, and Jacopo Chiggiato. Zooplankton diel vertical migration in the corsica channel (north-western
593 mediterranean sea) detected by a moored acoustic doppler current profiler. *Ocean Science*, 15(3):631–649, 2019.
- 594 James M Hamilton, Kate Collins, and Simon J Prinsenberg. Links between ocean properties, ice cover, and plankton
595 dynamics on interannual time scales in the canadian arctic archipelago. *Journal of Geophysical Research: Oceans*,
596 118(10):5625–5639, 2013.
- 597 Graeme C Hays. A review of the adaptive significance and ecosystem consequences of zooplankton diel vertical
598 migrations. In *Migrations and Dispersal of Marine Organisms: Proceedings of the 37 th European Marine Biology*
599 *Symposium held in Reykjavík, Iceland, 5–9 August 2002*, pages 163–170. Springer, 2003.
- 600 Karen J Heywood, S Scrope-Howe, and ED Barton. Estimation of zooplankton abundance from shipborne adcp
601 backscatter. *Deep Sea Research Part A. Oceanographic Research Papers*, 38(6):677–691, 1991.
- 602 Laura Hobbs, Neil S Banas, Jonathan H Cohen, Finlo R Cottier, Jørgen Berge, and Øystein Varpe. A marine
603 zooplankton community vertically structured by light across diel to interannual timescales. *Biology Letters*, 17(2):
604 20200810, 2021.
- 605 Raleigh R Hood, Lynnath E Beckley, and Jerry D Wiggert. Biogeochemical and ecological impacts of boundary
606 currents in the indian ocean. *Progress in Oceanography*, 156:290–325, 2017.
- 607 Raleigh R Hood, Victoria J Coles, Jenny A Huggett, Michael R Landry, Marina Levy, James W Moffett, and Timothy
608 Rixen. Nutrient, phytoplankton, and zooplankton variability in the indian ocean. In *The Indian Ocean and its*
609 *role in the global climate system*, pages 293–327. Elsevier, 2024.

- 610 Ryuichiro Inoue, Minoru Kitamura, and Tetsuichi Fujiki. Diel vertical migration of zooplankton at the s 1 biogeo-
611 chemical mooring revealed from acoustic backscattering strength. *Journal of Geophysical Research: Oceans*, 121
612 (2):1031–1050, 2016.
- 613 Songnian Jiang, Tommy D Dickey, Deborah K Steinberg, and Laurence P Madin. Temporal variability of zooplankton
614 biomass from adcp backscatter time series data at the bermuda testbed mooring site. *Deep Sea Research Part I:*
615 *Oceanographic Research Papers*, 54(4):608–636, 2007.
- 616 R Jyothibabu, NV Madhu, H Habeebrehman, KV Jayalakshmy, KKC Nair, and CT Achuthankutty. Re-evaluation
617 of ‘paradox of mesozooplankton’ in the eastern arabian sea based on ship and satellite observations. *Journal of*
618 *Marine Systems*, 81(3):235–251, 2010.
- 619 Myounghee Kang, Sunyoung Oh, Wooseok Oh, Dong-Jin Kang, SungHyun Nam, and Kyounghoon Lee. Acoustic
620 characterization of fish and macroplankton communities in the seychelles-chagos thermocline ridge of the southwest
621 indian ocean. *Deep Sea Research Part II: Topical Studies in Oceanography*, 213:105356, 2024.
- 622 Madhavan Girijakumari Keerthi, Matthieu Lengaigne, Marina Levy, Jerome Vialard, Vallivattathillam Parvathi,
623 Clément de Boyer Montégut, Christian Ethé, Olivier Aumont, Iyyappan Suresh, Valiya Parambil Akhil, et al.
624 Physical control of interannual variations of the winter chlorophyll bloom in the northern arabian sea. *Biogeosciences*, 14(15):3615–3632, 2017.
- 626 Punam A Khandagale, Vaibhav D Mhatre, and Sujitha Thomas. Seasonal and spatial variability of zooplankton
627 diversity in north eastern arabian sea along the maharashtra coast. *Journal of the Marine Biological Association*
628 *of India*, 64(1):25–32, 2022.
- 629 S Kidwai and S Amjad. Zooplankton: pre-southwest and northeast monsoons of 1993 to 1994, from the north arabian
630 sea. *Mar. Biol.*, 136(3):561–571, apr 2000.
- 631 Michael R Landry. Grazing processes and secondary production in the arabian sea: A simple food web synthesis
632 with measurement constraints. In *Indian Ocean Biogeochemical Processes and Ecological Variability*, Geophysical
633 monograph, pages 133–146. American Geophysical Union, Washington, D. C., 2009.
- 634 Corinne Le Qu, Robbie M Andrew, Josep G Canadell, Stephen Sitch, Jan Ivar Korsbakken, Glen P Peters, Andrew C
635 Manning, Thomas A Boden, Pieter P Tans, Richard A Houghton, et al. Global carbon budget 2016. *Earth System*
636 *Science Data*, 8(2):605–649, 2016.
- 637 Marina Lévy, D Shankar, J-M André, SSC Shenoi, Fabien Durand, and Clément de Boyer Montégut. Basin-wide
638 seasonal evolution of the indian ocean’s phytoplankton blooms. *Journal of Geophysical Research: Oceans*, 112
639 (C12), 2007.
- 640 M Li, A Gargett, and K Denman. What determines seasonal and interannual variability of phytoplankton and
641 zooplankton in strongly estuarine systems? *Estuarine, Coastal and Shelf Science*, 50(4):467–488, 2000.

- 642 Yanliang Liu, Jingsong Guo, Yuhuan Xue, Chalermrat Sangmanee, Huiwu Wang, Chang Zhao, Somkiat Khokiat-
643 tiwong, and Weidong Yu. Seasonal variation in diel vertical migration of zooplankton and micronekton in the
644 andaman sea observed by a moored adcp. *Deep Sea Research Part I: Oceanographic Research Papers*, 179:103663,
645 2022.
- 646 M Madhupratap, P Haridas, Neelam Ramaiah, and CT Achuthankutty. Zooplankton of the southwest coast of india:
647 abundance, composition, temporal and spatial variability in 1987. 1992.
- 648 M Madhupratap, TC Gopalakrishnan, P Haridas, KKC Nair, PN Aravindakshan, G Padmavati, and Shiney Paul.
649 Lack of seasonal and geographic variation in mesozooplankton biomass in the arabian sea and its structure in the
650 mixed layer. *Current science. Bangalore*, 71(11):863–868, 1996a.
- 651 M Madhupratap, S Prasanna Kumar, PMA Bhattathiri, M Dileep Kumar, S Raghukumar, KKC Nair, and N Rama-
652 iah. Mechanism of the biological response to winter cooling in the northeastern arabian sea. *Nature*, 384(6609):
653 549–552, 1996b.
- 654 M Madhupratap, TC Gopalakrishnan, P Haridas, and KKC Nair. Mesozooplankton biomass, composition and
655 distribution in the arabian sea during the fall intermonsoon: implications of oxygen gradients. *Deep Sea Research*
656 *Part II: Topical Studies in Oceanography*, 48(6-7):1345–1368, 2001.
- 657 John Marra and Richard T. Barber. Primary productivity in the arabian sea: A synthesis of jgofs data. *Progress*
658 *in Oceanography*, 65(2):159–175, 2005. ISSN 0079-6611. doi: <https://doi.org/10.1016/j.pocean.2005.03.004>. URL
659 <https://www.sciencedirect.com/science/article/pii/S007966110500042X>. The Arabian Sea of the 1990s: New
660 Biogeochemical Understanding.
- 661 JP McCreary, Raghu Murtugudde, Jerome Vialard, PN Vinayachandran, Jerry D Wiggert, Raleigh R Hood,
662 D Shankar, and S Shetye. Biophysical processes in the indian ocean. *Indian Ocean biogeochemical processes*
663 *and ecological variability*, 185:9–32, 2009.
- 664 Julian P McCreary Jr, Pijush K Kundu, and Robert L Molinari. A numerical investigation of dynamics, thermody-
665 namics and mixed-layer processes in the indian ocean. *Progress in Oceanography*, 31(3):181–244, 1993.
- 666 Julian P McCreary Jr, Kevin E Kohler, Raleigh R Hood, and Donald B Olson. A four-component ecosystem model
667 of biological activity in the arabian sea. *Progress in Oceanography*, 37(3-4):193–240, 1996.
- 668 S Mukhopadhyay, D Shankar, S G Aparna, and A Mukherjee. Observations of the sub-inertial, near-surface east
669 india coastal current. *Cont. Shelf Res.*, 148:159–177, September 2017.
- 670 KKC Nair, M Madhupratap, TC Gopalakrishnan, P Haridas, and Mangesh Gauns. The arabian sea: physical
671 environment, zooplankton and myctophid abundance. 1999.
- 672 PV Nair. Primary productivity in the indian seas. *CMFRI Bulletin*, 22:1–63, 1970.
- 673 D Nethery and D Shankar. Vertical propagation of baroclinic kelvin waves along the west coast of india. *J. Earth*
674 *Syst. Sci.*, 116(4):331–339, aug 2007.

- 675 Lingyun Nie, Jianchao Li, Hao Wu, Wenchao Zhang, Yongjun Tian, Yang Liu, Peng Sun, Zhenjiang Ye, Shuyang
676 Ma, and Qinfeng Gao. The influence of ocean processes on fine-scale changes in the yellow sea cold water mass
677 boundary area structure based on acoustic observations. *Remote Sensing*, 15(17):4272, 2023.
- 678 MD Ohman and H-J Hirche. Density-dependent mortality in an oceanic copepod population. *Nature*, 412(6847):
679 638–641, 2001.
- 680 SA Piontovski, R Williams, and TA Melnik. Spatial heterogeneity, biomass and size structure of plankton of the
681 indian ocean: some general trends. *Marine ecology progress series*, pages 219–227, 1995.
- 682 Emmanuel Potiris, Constantin Frangoulis, Alkiviadis Kalampokis, Manolis Ntoumas, Manos Pettas, George Peti-
683 hakis, and Vassilis Zervakis. Acoustic doppler current profiler observations of migration patterns of zooplankton
684 in the cretan sea. *Ocean Science*, 14(4):783–800, 2018.
- 685 SZ Qasim. Biological productivity of the indian ocean. 1977.
- 686 Seshagiri Raghukumar and AC Anil. Marine biodiversity and ecosystem functioning: A perspective. *Current Science*,
687 84(7):884–892, 2003.
- 688 CP Ramamirtham and AVS Murty. Hydrography of the west coast of india during the pre-monsoon period of the
689 year 1962—part 2: in and offshore waters of the konkan and malabar coasts. *Journal of the Marine Biological
690 Association of India*, 7(1):150–168, 1965.
- 691 S Ramamurthy. Studies on the plankton of the north kanara coast in relation to the pelagic fishery. *Journal of
692 Marine Biological Association of India*, 7(1):127–149, 1965.
- 693 M Reckermann and M J W Veldhuis. Trophic interactions between picophytoplankton and micro- and nanozoo-
694 plankton in the western arabian sea during the NE monsoon 1993. *Aquat. Microb. Ecol.*, 12:263–273, 1997.
- 695 Mehbuba Rehim and Mudassar Imran. Dynamical analysis of a delay model of phytoplankton–zooplankton interac-
696 tion. *Applied Mathematical Modelling*, 36(2):638–647, 2012.
- 697 T. P. Rippeth and J. H. Simpson. Diurnal signals in vertical motions on the hebridean shelf. *Limnology and
698 Oceanography*, 43:1690–1696, 1998. doi: 10.4319/lo.1998.43.7.1690.
- 699 William J Ripple, James A Estes, Oswald J Schmitz, Vanessa Constant, Matthew J Kaylor, Adam Lenz, Jennifer L
700 Motley, Katharine E Self, David S Taylor, and Christopher Wolf. What is a trophic cascade? *Trends Ecol. Evol.*,
701 31(11):842–849, November 2016.
- 702 John H Ryther, John R Hall, Allan K Pease, Andrew Bakun, and Mark M Jones. Primary organic production in
703 relation to the chemistry and hydrography of the western indian ocean 1. *Limnology and Oceanography*, 11(3):
704 371–380, 1966.
- 705 Kankan Sarkar, SG Aparna, Shrikant Dora, and D Shankar. Seasonal variability of sea-surface temperature fronts
706 associated with large marine ecosystems in the north indian ocean. *Journal of Earth System Science*, 128(1):20,
707 2019.

- 708 VVSS Sarma, DV Desai, JS Patil, L Khandeparker, SG Aparna, D Shankar, Selrina D'Souza, HB Dalabehera,
709 J Mukherjee, P Sudharani, et al. Ecosystem response in temperature fronts in the northeastern arabian sea.
710 *Progress in Oceanography*, 165:317–331, 2018.
- 711 D Shankar, SSC Shenoi, RK Nayak, PN Vinayachandran, G Nampoothiri, AM Almeida, GS Michael, MR Ramesh
712 Kumar, D Sundar, and OP Sreejith. Hydrography of the eastern arabian sea during summer monsoon 2002.
713 *Journal of earth system science*, 114:459–474, 2005.
- 714 D Shankar, R Remya, PN Vinayachandran, Abhisek Chatterjee, and Ambica Behera. Inhibition of mixed-layer
715 deepening during winter in the northeastern arabian sea by the west india coastal current. *Climate Dynamics*,
716 47:1049–1072, 2016.
- 717 D Shankar, R Remya, AC Anil, and V Vijith. Role of physical processes in determining the nature of fisheries in the
718 eastern arabian sea. *Progress in Oceanography*, 172:124–158, 2019.
- 719 SSC Shenoi, D Shankar, GS Michael, J Kurian, KK Varma, MR Ramesh Kumar, AM Almeida, AS Unnikrishnan,
720 W Fernandes, N Barreto, et al. Hydrography and water masses in the southeastern arabian sea during march–june
721 2003. *Journal of earth system science*, 114:475–491, 2005.
- 722 SR Shetye, AD Gouveia, SSC Shenoi, D Sundar, GS Michael, AM Almeida, and K Santanam. Hydrography and
723 circulation off the west coast of india during the southwest monsoon 1987. 1990.
- 724 SR Shetye, AD Gouveia, and SSC Shenoi. Does winter cooling lead to the subsurface salinity minimum off saurashtra,
725 india? *Oceanography of the Indian Ocean*, pages 617–625, 1992.
- 726 Wei Shi and Menghua Wang. Phytoplankton biomass dynamics in the arabian sea from viirs observations. *Journal
727 of Marine Systems*, 227:103670, 2022.
- 728 Houssem Smeti, Marc Pagano, Christophe Menkes, Anne Lebourges-Dhaussy, Brian PV Hunt, Valerie Allain, Martine
729 Rodier, Florian De Boissieu, Elodie Kestenare, and Cherif Sammari. Spatial and temporal variability of zooplankton
730 off n ew c aledonia (s outhwestern p acific) from acoustics and net measurements. *Journal of Geophysical
731 Research: Oceans*, 120(4):2676–2700, 2015.
- 732 Sharon Smith, Michael Roman, Irina Prusova, Karen Wishner, Marcia Gowing, LA Codispoti, Richard Barber, John
733 Marra, and Charles Flagg. Seasonal response of zooplankton to monsoonal reversals in the arabian sea. *Deep Sea
734 Research Part II: Topical Studies in Oceanography*, 45(10-11):2369–2403, 1998.
- 735 SL Smith and M Madhupratap. Mesozooplankton of the arabian sea: patterns influenced by seasons, upwelling, and
736 oxygen concentrations. *Progress in Oceanography*, 65(2-4):214–239, 2005.
- 737 Patnaik Sreenivas, KVKRK Patnaik, and KVSR Prasad. Monthly variability of mixed layer over arabian sea using
738 argo data. *Marine Geodesy*, 31(1):17–38, 2008.

- 739 R Subrahmanyam. Studies on the phytoplankton of the west coast of india: Part ii. physical and chemical factors
740 influencing the production of phytoplankton, with remarks on the cycle of nutrients and on the relationship of
741 the phosphate-content to fish landings. In *Proceedings/Indian Academy of Sciences*, volume 50, pages 189–252.
742 Springer, 1959.
- 743 R Subrahmanyam and AH Sarma. Studies on the phytoplankton of the west coast of india. part iii. seasonal variation
744 of the phytoplankters and environmental factors. *Indian Journal of Fisheries*, 7(2):307–336, 1960.
- 745 Laura Ursella, Vanessa Cardin, Mirna Batistić, Rade Garić, and Miroslav Gačić. Evidence of zooplankton vertical
746 migration from continuous southern adriatic buoy current-meter records. *Progress in oceanography*, 167:78–96,
747 2018.
- 748 Laura Ursella, Sara Pensieri, Enric Pallàs-Sanz, Sharon Z Herzka, Roberto Bozzano, Miguel Tenreiro, Vanessa Cardin,
749 Julio Candela, and Julio Sheinbaum. Diel, lunar and seasonal vertical migration in the deep western gulf of mexico
750 evidenced from a long-term data series of acoustic backscatter. *Progress in Oceanography*, 195:102562, 2021.
- 751 V Vijith, PN Vinayachandran, V Thushara, P Amol, D Shankar, and AC Anil. Consequences of inhibition of mixed-
752 layer deepening by the west india coastal current for winter phytoplankton bloom in the northeastern arabian sea.
753 *Journal of Geophysical Research: Oceans*, 121(9):6583–6603, 2016.
- 754 Peter H Wiebe, Charles H Greene, Timothy K Stanton, and Janusz Burczynski. Sound scattering by live zooplankton
755 and micronekton: empirical studies with a dual-beam acoustical system. *The Journal of the Acoustical Society of
756 America*, 88(5):2346–2360, 1990.
- 757 Jerry D Wiggert, RR Hood, Karl Banse, and JC Kindle. Monsoon-driven biogeochemical processes in the arabian
758 sea. *Progress in Oceanography*, 65(2-4):176–213, 2005.
- 759 Monika Winder and Daniel E Schindler. Climatic effects on the phenology of lake processes. *Global change biology*,
760 10(11):1844–1856, 2004.
- 761 Karen F Wishner, Marcia M Gowing, and Celia Gelfman. Mesozooplankton biomass in the upper 1000 m in the
762 arabian sea: overall seasonal and geographic patterns, and relationship to oxygen gradients. *Deep Sea Research
763 Part II: Topical Studies in Oceanography*, 45(10-11):2405–2432, 1998.

Table 1: ADCP deployment details at the locations. The temporal resolution is 1 hour, bin size(vertical resolution) 4 m. All ADCPs are operated at 153.3 kHz. The moorings are at a water column depth of 950–1200 m on the continental slope and are serviced on yearly basis according to ship availability. The 6th column consists of Reference echo intensity (Er) for each beam, while the 7th column contains the corresponding RSSI conversion factor [Deines, 1999].

Station (Position; $^{\circ}$ E, $^{\circ}$ N)	Date		Depth			
	Deployment	Recovery	Ocean	ADCP	Er	Kc
Okha (67.47, 22.26)	01/10/2018	01/12/2019	996	118	37 , 37 , 37 , 36	0.42 , 0.44 , 0.42 , 0.43
	01/12/2019	04/12/2020	1166	312	39 , 36 , 38 , 36	0.42 , 0.44 , 0.42 , 0.43
	04/12/2020	08/03/2022	1021	144	41 , 37 , 38 , 37	0.42 , 0.44 , 0.42 , 0.43
	08/03/2022	01/01/2023	1019	142	37 , 38 , 39 , 36	0.42 , 0.44 , 0.42 , 0.43
Mumbai (69.24, 20.01)	09/11/2017	29/09/2018	1025	150	36 , 34 , 39 , 42	0.40 , 0.40 , 0.40 , 0.40
	29/09/2018	29/11/2019	1122	125	35 , 36 , 39 , 42	0.40 , 0.40 , 0.40 , 0.40
	29/11/2019	02/12/2020	1143	164	37 , 34 , 39 , 43	0.40 , 0.40 , 0.40 , 0.40
	02/12/2020	06/03/2022	1125	142	36 , 34 , 39 , 42	0.40 , 0.40 , 0.40 , 0.40
	07/03/2022	02/01/2023	1103	158	37 , 34 , 40 , 43	0.40 , 0.40 , 0.40 , 0.40
Jaigarh (71.12, 17.53)	27/10/2017	27/09/2018	1039	198	32 , 35 , 33 , 32	0.45 , 0.45 , 0.45 , 0.45
	27/09/2018	30/10/2019	1032	164	32 , 35 , 33 , 31	0.45 , 0.45 , 0.45 , 0.45
	03/11/2019	30/11/2020	1142	264	32 , 36 , 33 , 32	0.45 , 0.45 , 0.45 , 0.45
	30/11/2020	05/03/2022	1099	119	33 , 36 , 34 , 32	0.45 , 0.45 , 0.45 , 0.45
Goa (72.74, 15.17)	03/10/2017	25/09/2018	1000	174	35 , 37 , 34 , 35	0.44 , 0.44 , 0.40 , 0.41
	25/09/2018	16/10/2019	969	145	38 , 36 , 36 , 34	0.44 , 0.44 , 0.40 , 0.41
	16/10/2019	29/11/2020	966	143	44 , 38 , 36 , 43	0.44 , 0.44 , 0.40 , 0.41
	29/11/2020	03/03/2022	985	157	35 , 40 , 35 , 38	0.44 , 0.44 , 0.40 , 0.41
	03/03/2022	05/01/2023	984	159	35 , 38 , 35 , 34	0.44 , 0.44 , 0.40 , 0.41
Udupi (74.04, 12.5)	05/10/2017	06/10/2018	1028	176	44 , 46 , 29 , 35	0.45 , 0.45 , 0.45 , 0.45
	06/10/2018	18/10/2019	1027	179	32 , 38 , 30 , 36	0.45 , 0.45 , 0.45 , 0.45
	18/10/2019	11/12/2020	1018	168	33 , 37 , 31 , 38	0.45 , 0.45 , 0.45 , 0.45
	11/03/2022	06/01/2023	1036	155	31 , 32 , 32 , 33	0.45 , 0.45 , 0.45 , 0.45
Kollam (75.44, 9.05)	07/10/2017	08/10/2018	1174	200	43 , 55 , 45 , 43	0.49 , 0.50 , 0.49 , 0.50
	08/10/2018	20/10/2019	1160	123	49 , 62 , 46 , 46	0.49 , 0.50 , 0.49 , 0.50
	20/10/2019	13/12/2020	1209	176	52 , 61 , 54 , 55	0.49 , 0.50 , 0.49 , 0.50
	13/12/2020	13/03/2022	1129	91	49 , 51 , 46 , 47	0.49 , 0.50 , 0.49 , 0.50
	13/03/2022	08/01/2023	1149	164	41 , 48 , 43 , 41	0.49 , 0.50 , 0.49 , 0.50
Kanyakumari (77.39, 6.96)	16/11/2016	08/10/2017	1096	252	37 , 36 , 37 , 37	0.42 , 0.44 , 0.42 , 0.43
	08/10/2017	10/10/2018	1055	181	32 , 34 , 38 , 35	0.45 , 0.45 , 0.45 , 0.45
	10/10/2018	22/10/2019	1075	180	36 , 34 , 39 , 36	0.45 , 0.45 , 0.45 , 0.45
	22/10/2019	14/12/2020	1060	167	33 , 35 , 36 , 35	0.45 , 0.45 , 0.45 , 0.45
	14/12/2020	14/03/2022	1184	287	34 , 36 , 36 , 35	0.45 , 0.45 , 0.45 , 0.45

Table 2:

Volumetric samples of zooplankton of various stations. The sampling depth range is standardised for later years for bin range of 0–25m, 25–50m, 50–75m, 75–100m, 100–150m. The abbreviations are in the following manner: Okha (O), Mumbai (M), Jaigarh (J), Goa (G), Udupi (U), Kollam (K), Kanyakumari (KK); The number tags corresponds to particular cruise of a station.

Sample number	Tag	Lat($^{\circ}$ N)	Lon($^{\circ}$ E)	Date	Time (IST)	Sampling depth range (m)
1-3	G1	15.18	72.79	25 Sep 18	452	50–25, 100–50, 150–100
4-6	G2	15.16	72.71	25 Sep 18	2108	50–25, 100–50, 150–100
7-10	G2	15.16	72.71	25 Sep 18	2137	40–20, 60–40, 80–60, 100–80
11-14	J1			26 Sep 18	2000	40–20, 60–40, 80–60, 100–80
15-17	J2			27 Sep 18	2000	50–25, 100–50, 150–100
18-21	J2			27 Sep 18	2100	40–20, 60–40, 80–60, 100–80
22-25	M1	20	69.19	28 Sep 18	2135	40–20, 60–40, 80–60, 100–80
26-27	M1	20	69.19	28 Sep 18	2205	50–25, 100–50
28-29	M2	20.01	69.2	29 Sep 18	2035	50–25, 100–50
30-33	M2	20.01	69.2	29 Sep 18	2057	40–20, 60–40, 80–60, 100–80
34-37	U1			5 Oct 18	2000	40–20, 60–40, 80–60, 100–80
38-40	U1			5 Oct 18	2100	50–25, 100–50, 150–100
41-43	U2			6 Oct 18	2000	50–25, 100–50, 150–100
44-47	U2			6 Oct 18	2100	40–20, 60–40, 80–60, 100–80
48-51	K1	9.06	75.42	8 Oct 18	421	40–20, 60–40, 80–60, 100–80
52-54	K1	9.06	75.42	8 Oct 18	449	50–25, 100–50, 150–100
55-56	K2	9.04	75.4	8 Oct 18	2027	50–25, 100–50
57-60	K2	9.04	75.4	8 Oct 18	2045	40–20, 60–40, 80–60, 100–80
61-64	G2	15.16	72.74	16 Oct 19	829	50–25, 75–50, 100–75, 150–100
65-67	G3	15.16	72.74	16 Oct 19	1812	50–25, 75–50, 100–75
68-70	K2	9.02	75.42	20 Oct 19	840	50–25, 75–50, 100–75
71-74	K3	9.04	75.43	20 Oct 19	1934	50–25, 75–50, 100–75, 150–100
75-78	KK1			22 Oct 19	742	50–25, 75–50, 100–75, 150–100
79-82	KK2			22 Oct 19	1925	50–25, 75–50, 100–75, 150–100
83-86	J1			30 Oct 19	324	50–25, 75–50, 100–75, 150–100
87-89	J2			4 Nov 19	946	75–50, 100–75, 150–100
90-92	M2	19.98	69.22	29 Nov 19	1434	50–25, 75–50, 100–75
93-96	M3	20.01	69.23	30 Nov 19	958	50–25, 75–50, 100–75, 150–100
97-100	O1	22.24	67.49	1 Dec 19	937	50–25, 75–50, 100–75, 150–100
101	O2	22.25	67.46	1 Dec 19	1957	150–100
102-105	G3	15.68	73.22	28 Nov 20	930	50–25, 75–50, 100–75, 150–100
105-108	G4	15.32	73.22	29 Nov 20	1558	50–25, 75–50, 100–75, 150–100
108-110	J2	17.85	71.21	30 Nov 20	1458	75–50, 100–75, 150–100
111-114	J3	17.91	71.21	1 Dec 20	1052	50–25, 75–50, 100–75, 150–100
115-118	M4	20.03	69.38	2 Dec 20	2016	50–25, 75–50, 100–75, 150–100
119-00	O2	22.41	67.8	4 Dec 20	953	150–100
120-123	O3	22.41	67.79	4 Dec 20	2011	50–25, 75–50, 100–75, 150–100
124-127	K3	9.11	75.72	12 Dec 20	2335	50–25, 75–50, 100–75, 150–100
128-131	K4	9.06	75.74	13 Dec 20	1507	50–25, 75–50, 100–75, 150–100
132-134	KK1	7.62	77.63	14 Dec 20	1226	50–25, 75–50
135-138	KK2	7.62	77.63	14 Dec 20	2047	50–25, 75–50, 100–75, 150–100
139-142	G4	15.32	73.21	3 Mar 22	823	50–25, 75–50, 100–75, 150–100
143-146	G5	15.68	73.21	4 Mar 22	1030	50–25, 75–50, 100–75, 150–100
147-150	M5	19.99	69.23	7 Mar 22	957	50–25, 75–50, 100–75, 150–100
151-154	O3	22.24	67.5	8 Mar 22	806	50–25, 75–50, 100–75, 150–100
155-158	U3	12.5	74.04	12 Mar 22	1156	50–25, 75–50, 100–75, 150–100
159-160	K4	9.04	75.42	13 Mar 22	1027	50–25, 75–50, 100–75
161-164	KK3	6.97	77.4	15 Mar 22	1220	50–25, 75–50, 100–75, 150–100

Table 3:

The mean, standard deviation at 40 and 104 m of zooplankton biomass (mg m^{-3}), standard deviation of ZSS (gm m^{-2} , 0–140 m) and chlorophyll (mg m^{-3}) at 7 mooring sites are tabulated along with the standard deviation of components of biomass variability, namely intraseasonal, intra-annual and annual. The standard deviation, 3σ of Chl and ZSS is based on the monthly climatological data while the rest are based on the respective daily data.

	40 m biomass		104 m biomass		decrease with depth (40m – 104m)	standard deviation * 3				
	Mean	Std	Mean	Std		Chl	ZSS	Intraseasonal	Intra-annual	Annual
Okha	230.42	22.84	151.68	25.58	78.74	0.76	5.8	64.26	63.78	22.38
Mumbai	272.86	34.95	182.24	30.34	90.62	0.4	8.69	70.74	83.52	41.58
Jaigarh	278.45	36.52	182.96	48.89	95.49	0.15	9.72	90.3	87.06	54.3
Goa	235.22	30.34	163.02	36.54	72.2	0.45	6.72	76.38	83.76	38.58
Udupi	247.81	34.37	169.37	38.8	78.43	1.65	6.01	77.22	100.86	41.64
Kollam	272.56	54.94	198.89	50.08	73.67	2.05	3.75	89.94	95.94	41.82
KanyaKumari	207.07	30.42	167.63	20.89	39.44	1.53	2.02	71.88	52.62	21.84

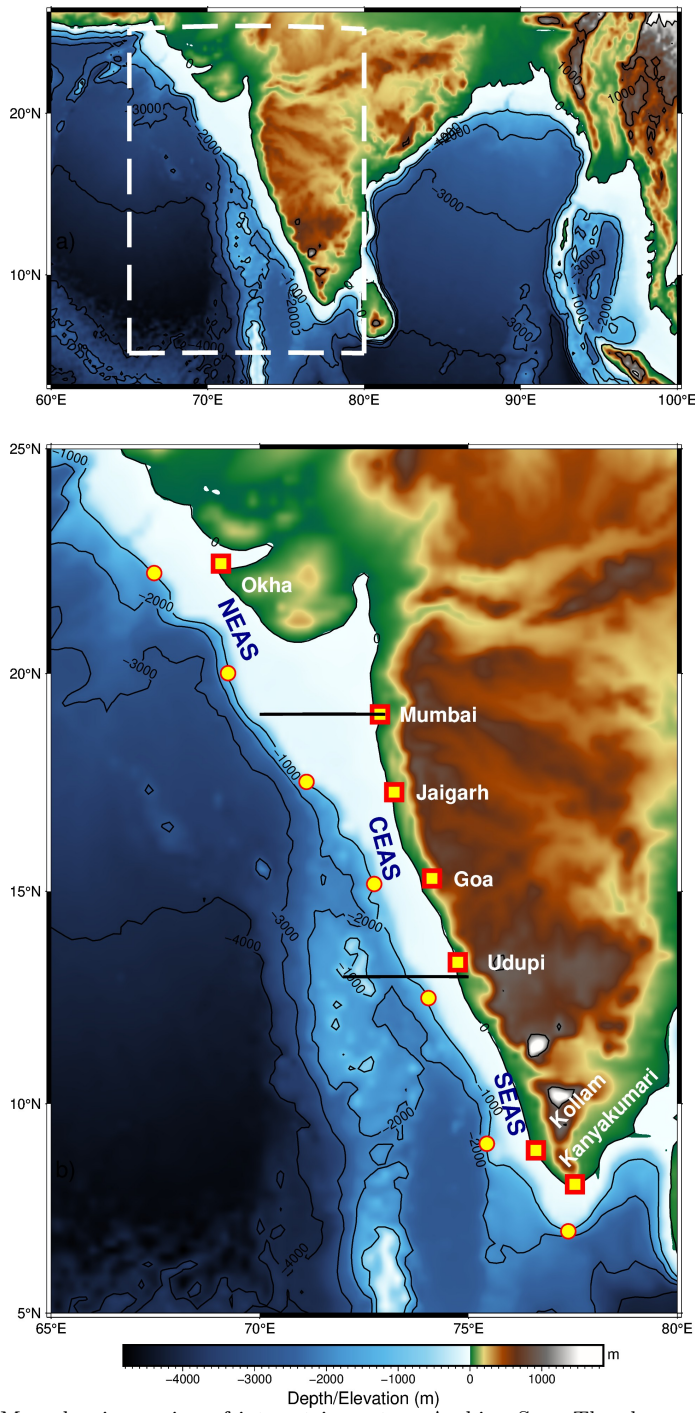


Figure 1: Map showing region of interest in eastern Arabian Sea. The slope moorings are deployed at ~ 1000 m depth as shown in the bathymetry contour. Note the increase in shelf width as we go poleward along the coast. The mooring sites off Okha and Mumbai are in Northern EAS; Jaigarh and Goa in Central EAS while Kollam and Kanyakumari are at Southern EAS. Udupi is situated at the transition zone of Central and Southern EAS.

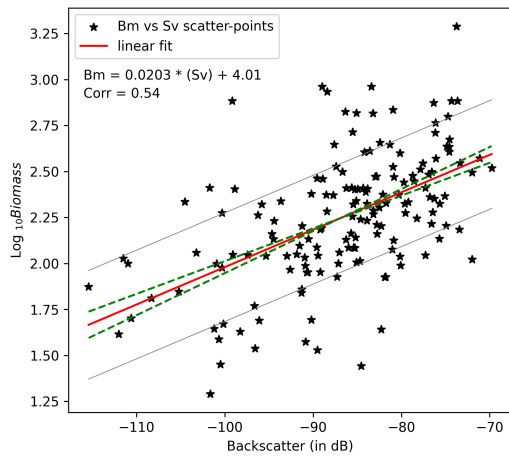


Figure 2: The linear fit line of Biomass (\log_{10} scale) and backscattering strength (in dB). The linear fit line is within the error range of previous result of [Aparna et al., 2022] (contained 67 data points) onto which latest zooplankton volumetric sample data (159 data points) is appended. The regression equation is $y = (0.02 \pm 0.0025) x + (4.0144 \pm 0.2198)$ and correlation value of 0.54. The dashed green lines denote error range of plausible slope and intercept. From the linear equation, the upper and lower bound of error limit leads to an error bar of $\sim 14 \text{ mg m}^{-3}$. The first standard deviation of $\log_{10}(\text{Biomass})$ is ± 0.49 , which results in the backscatter range of 48.58 dB encompassing the entire backscatter range. It signifies the robustness of zooplankton biomass dependency on ADCP measured backscattering strength.

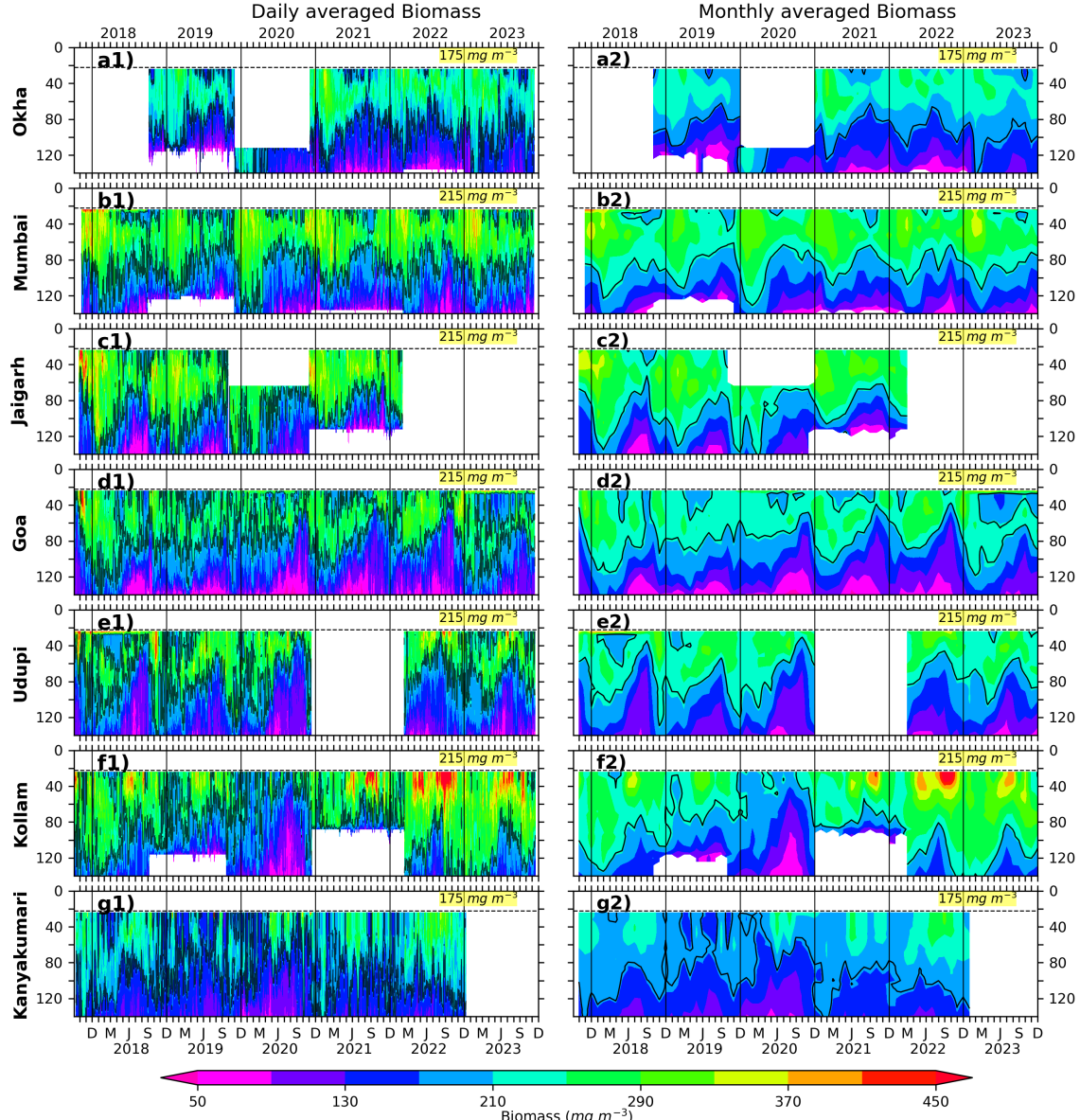


Figure 3: The Daily and monthly averaged biomass for EAS moorings, north (top) to south (bottom). The black contours are marking of 175 mg m^{-3} biomass for Okha and Kanyakumari; 215 mg m^{-3} for Mumbai, Goa and Kollam. The biomass contours are distinct and different based on the physico-chemical parameters and the one that best explains seasonality at respective location. The top 10 % of data is discarded due to echo noise. The dashed line at 22 m marks the top-depth of first bin i.e, 24 m.

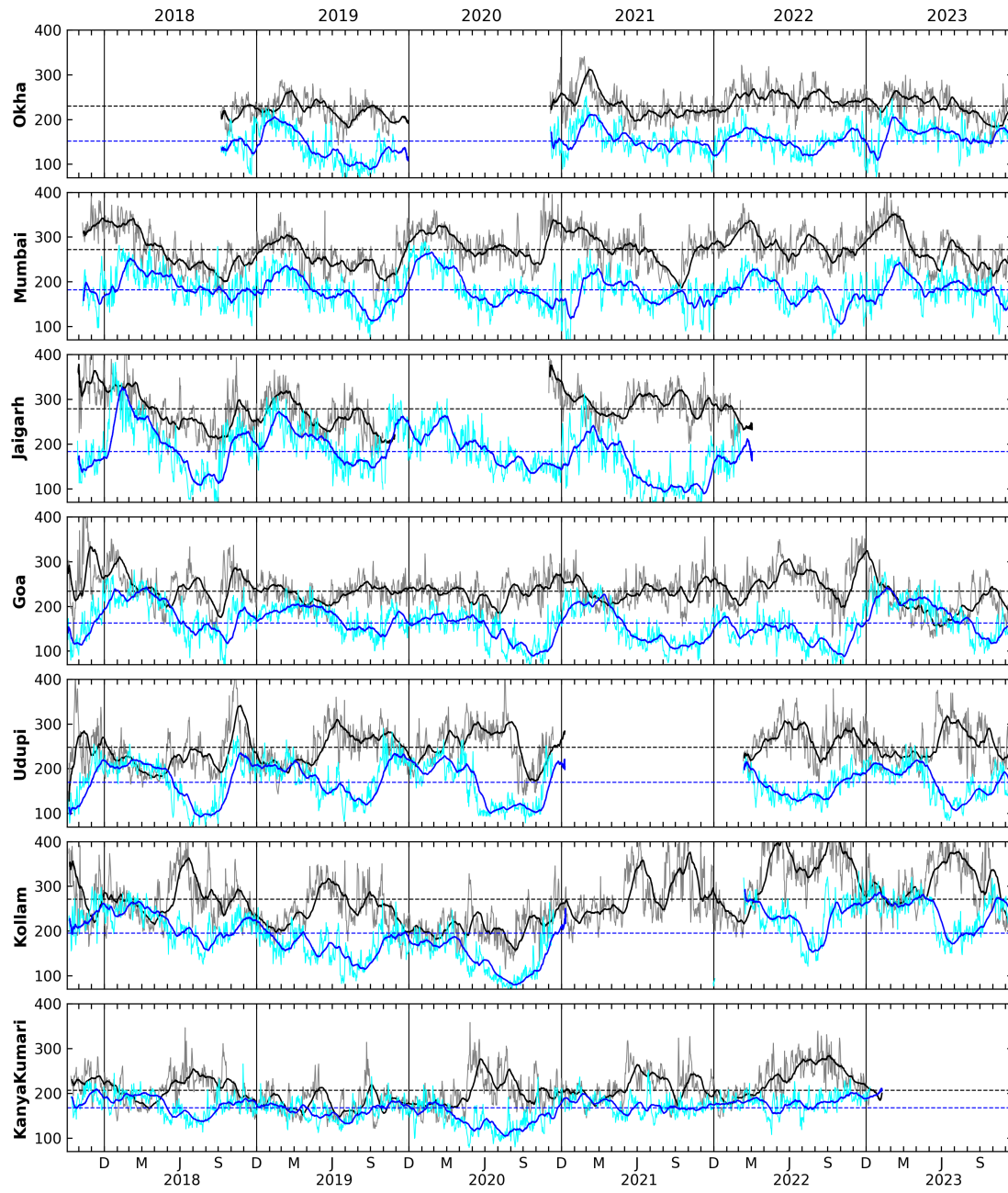


Figure 4: The daily biomass at depth of 40 m and 104 m for all locations shown by grey and cyan curves. The black and blue lines shows the 30 day rolling averaged biomass at 40 and 104 m, respectively. Notice the bursts seen in the daily data ranging from few days to weeks.

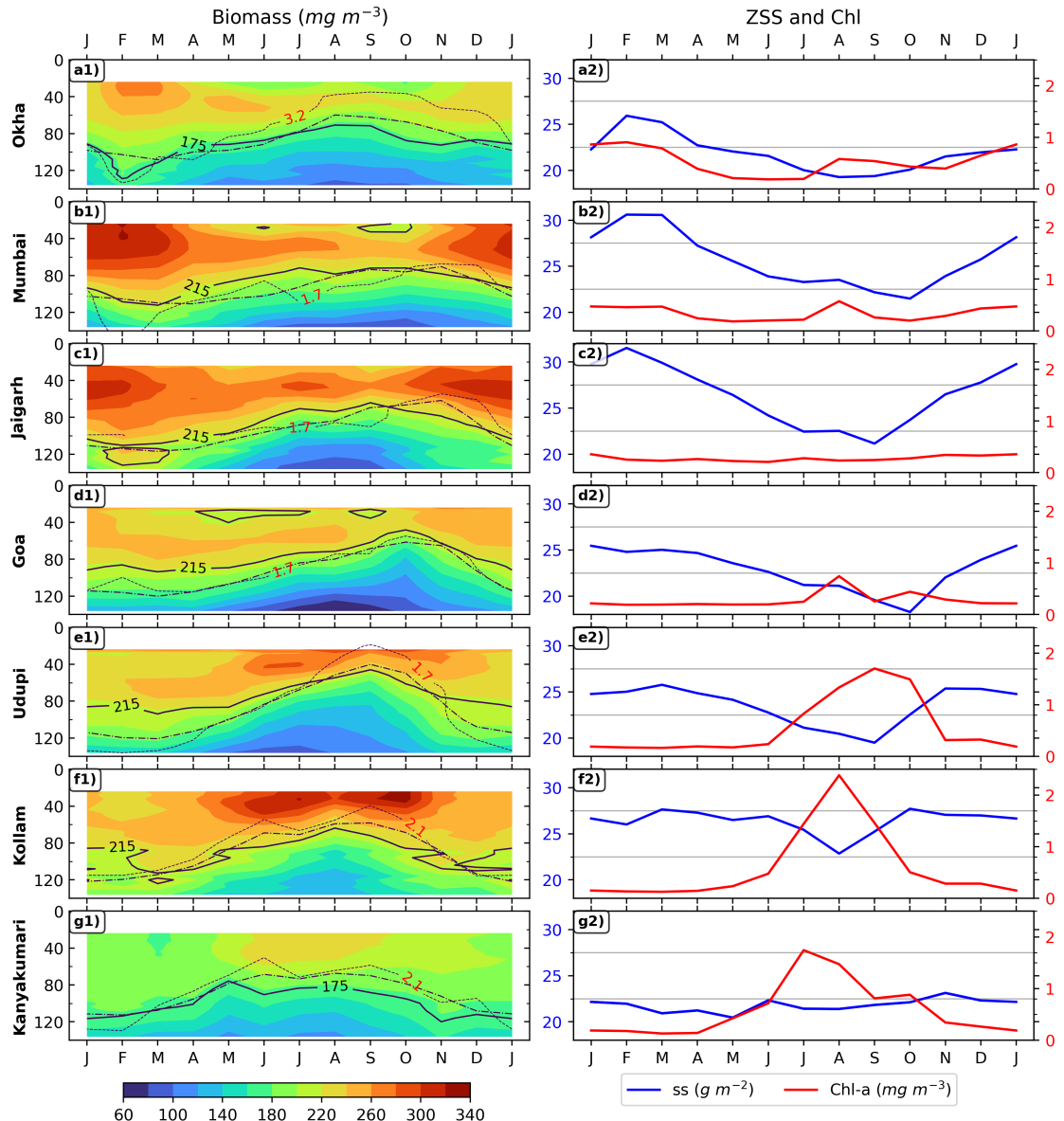


Figure 5: Monthly climatology of zooplankton biomass is shown in left panels for 7 locations, (top to bottom is southward). The D175 and D215 are shown in solid lines; dashed line represents the depth of 23 C isotherm; oxygen contours are shown in dotted lines and labeled for each mooring. The right set of panel plots is showing ZSS (24–140 biomass integral) and chlorophyll climatology for corresponding locations.

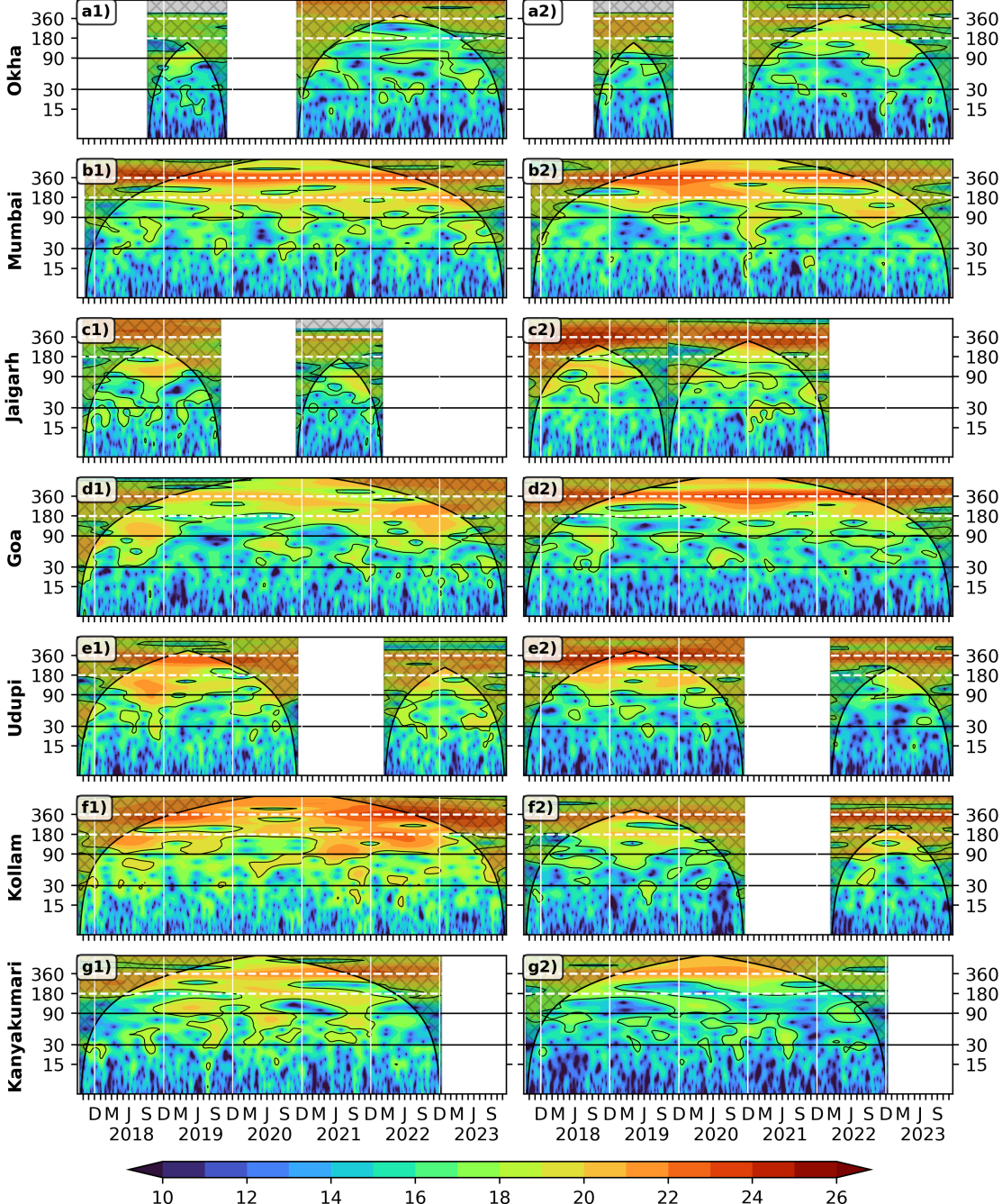


Figure 6: Wavelet power spectra (Morlet) of the 40 m (left panel) and 104 m (right panel) zooplankton biomass plotted against time as abscissa and period in days as ordinate. The wavelet power is in \log_2 scale, the 95 % significance is marked in black contours; the cross-shaded region falls under cone of influence. Vertical white lines separates years.

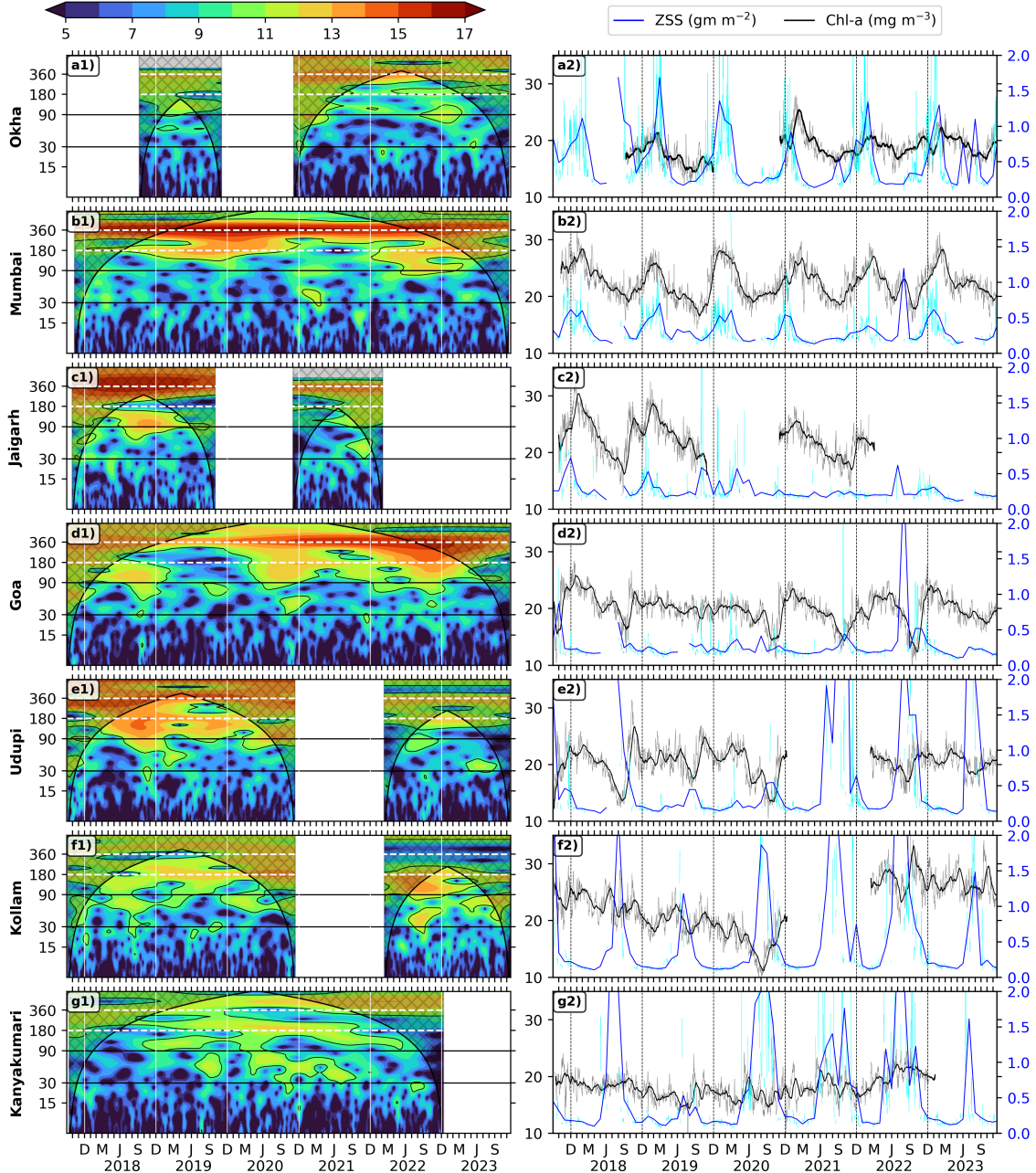


Figure 7: Wavelet power spectra (Morlet) of zooplankton standing stock plotted against time as abscissa and period in days as ordinate. The wavelet power is in log₂ scale, the 95 % significance is marked in black contours; The vertical white lines separates years. The right side panel shows the ZSS (24–120 m biomass integral) time series of 30 day rolling mean data (black) overlaid upon daily data (Grey). The 30 day rolling mean data of chlorophyll (solid blue) is plotted over its daily data (cyan).

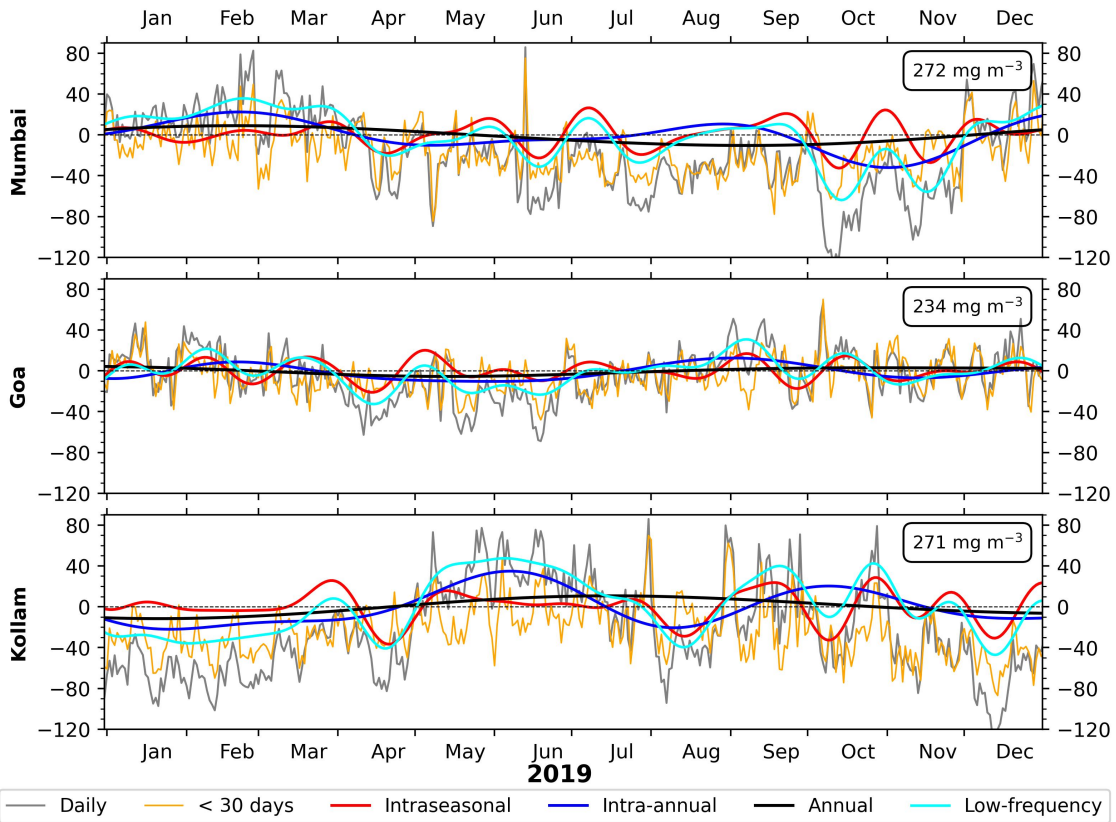


Figure 8: Comparison between mean-removed daily biomass time series at 40 m and the distinct components of variability off Mumbai, Goa and Kollam for 2019. The biomass units are mg m^{-3} and its mean for respective location is shown in top right box. The cyan curve is sum of all low frequency components above 30 days, i.e, annual, intra-annual and 30 to 90 days intraseasonal variability. Off Mumbai and Kollam, an increase in biomass is noticed from May onward and lasting till late monsoon with weeks of low biomass during August due to contribution from each component of variability.

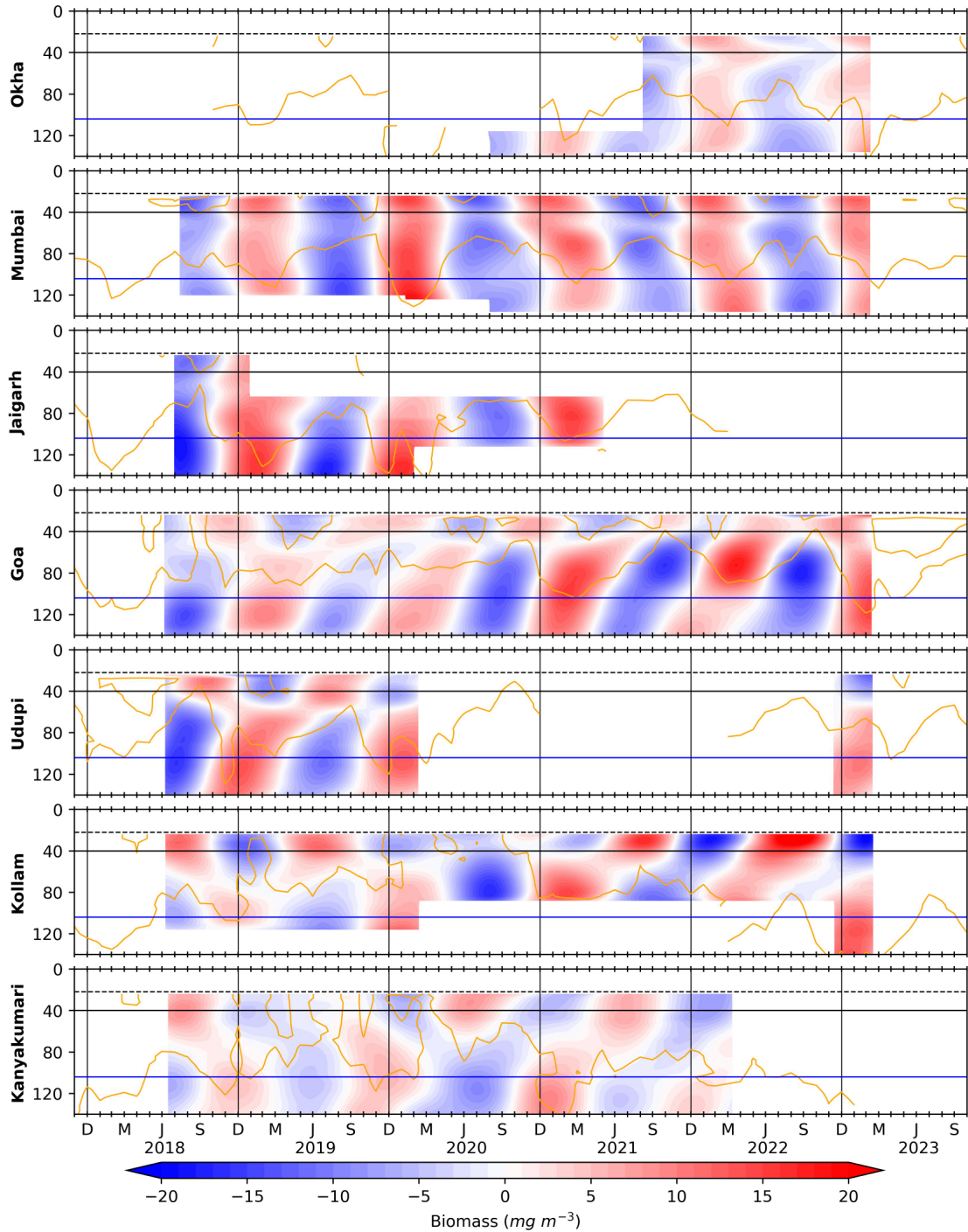


Figure 9: The biomass variation occurring in annual band (300 to 400 days). Owing to the presence of monsoon, there is a variation driven by associated upwelling (downwelling) processes in summer (winter) monsoon. and The horizontal black and blue lines is for 40 and 104 m respectively; vertical black lines separate the years. The dashed line at 22 m marks the top-depth of first bin i.e, 24 m ⁴⁵ and solid orange curves denotes D215 (D175 off Okha and Kanyakumari)

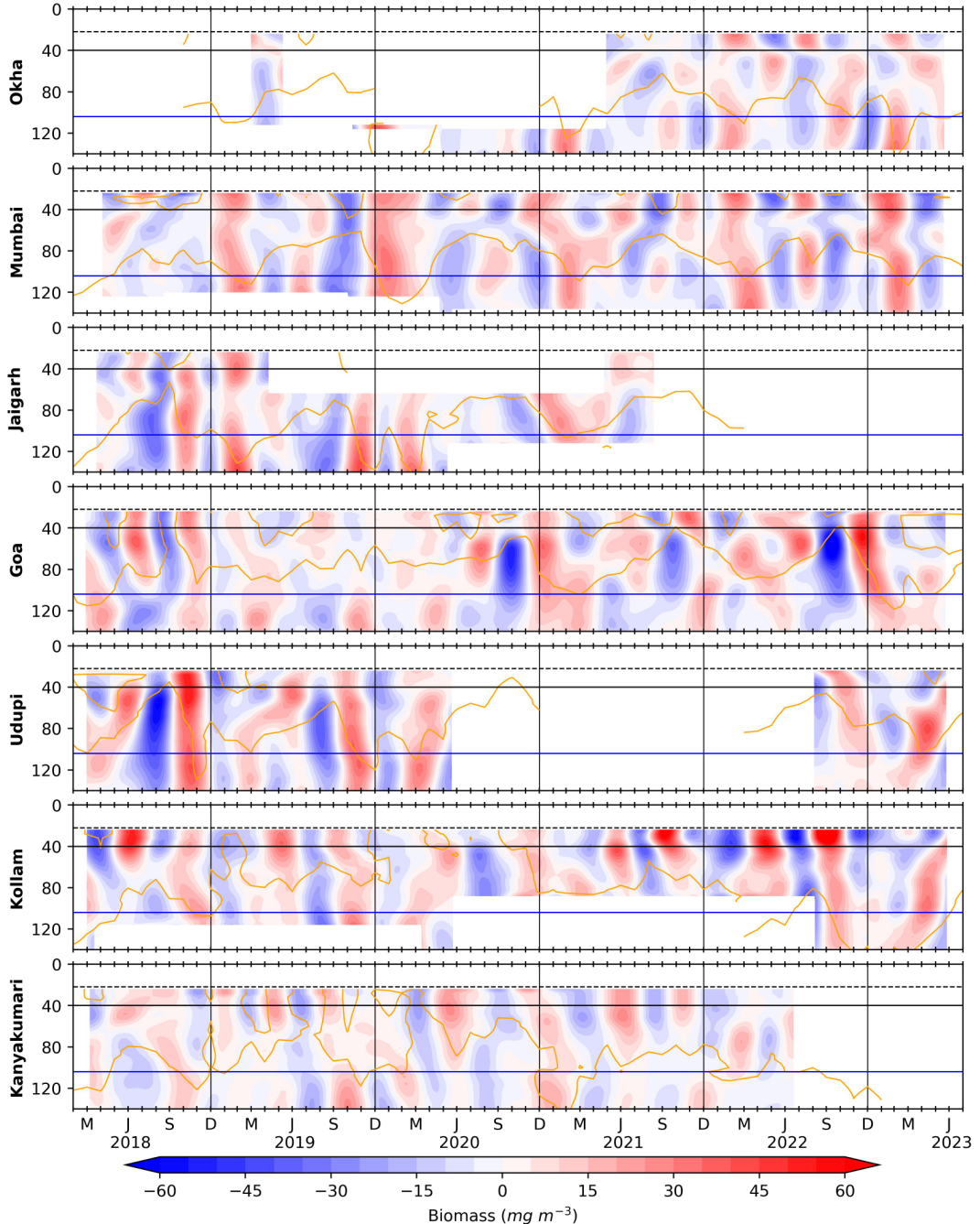


Figure 10: The biomass variation occurring in 100 to 250 days period (between the seasons and within a year record or intra-annual band) is obtained using a band pass filter. The horizontal black and blue lines is for 40 and 104 m respectively; vertical black lines separate the years. The dashed line at 22 m marks the top-depth of first bin i.e, 24 m and solid orange curves denotes D215 (D175 off Okha and Kanyakumari).

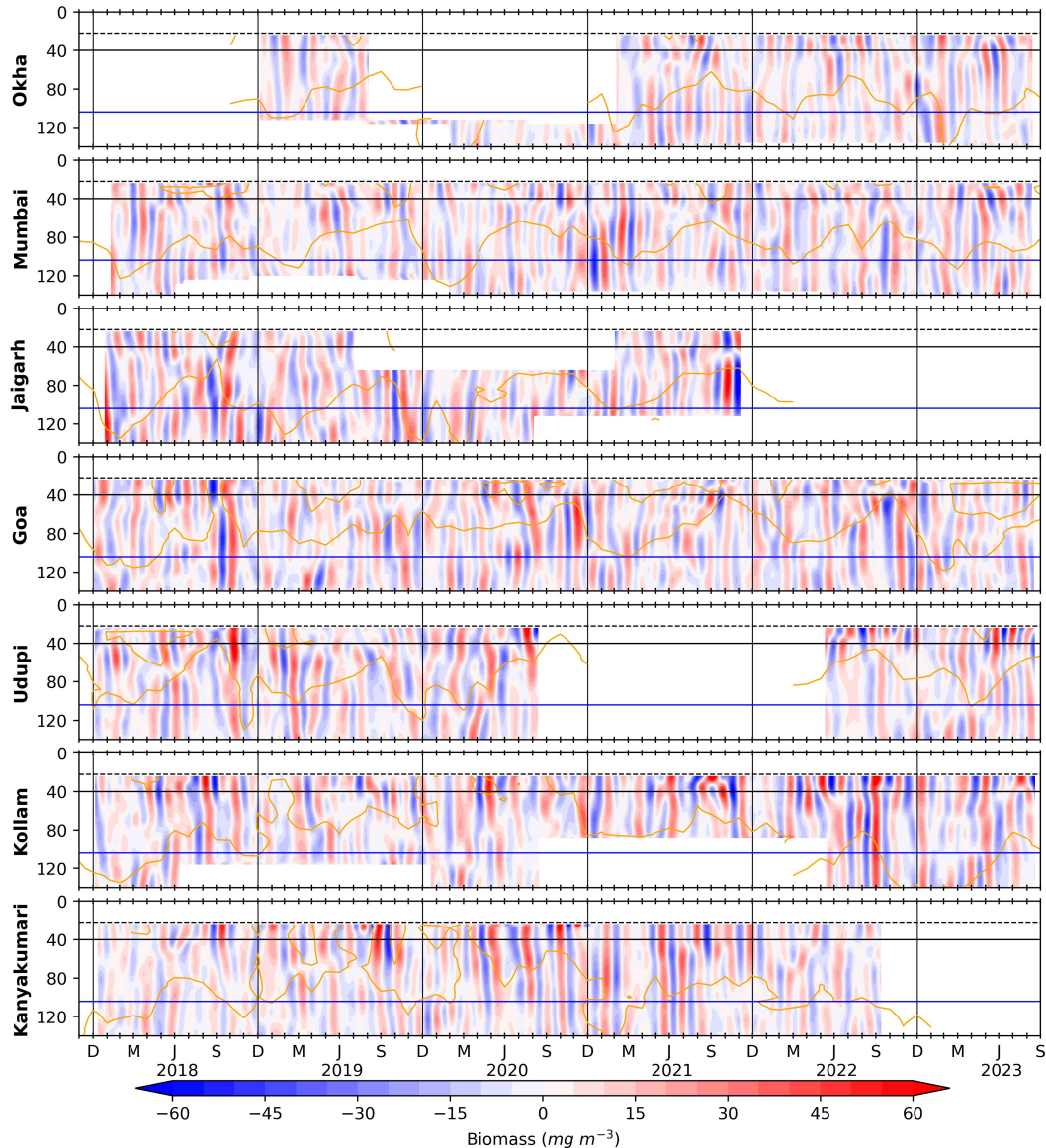


Figure 11: Biomass variation found in the Intraseasonal band i.e., 30 to 90 days period is obtained using a lanczos band pass filter. The horizontal black and blue lines is for 40 and 104 m respectively; vertical black lines separate the years and solid orange curves denotes D215 (D175 off Okha and Kanyakumari). The dashed line at 22 m marks the top-depth of first bin i.e, 24 m. Intraseasonal variability is seen throughout the record, is coherent along the slope and its magnitude is stronger during August to November.